International Journal of Innovative Scientific & Engineering Technologies Research 14(1):67-96, Jan-Mar., 2026

© SEAHI PUBLICATIONS, 2026 www.seahipublications.org ISSN: 2360-896X

doi:10.5281/zenodo.18415271

Reliability Analysis Of Reinforced Concrete Transmission Power Poles Subjected To Wind Load In Port Harcourt, Rivers State

Wojile, P. I., Sule, S & Awodiji C.T.G

Department of Civil Engineering,
Faculty of Engineering
University of Port Harcourt, Port Harcourt, Nigeria
Corresponding author email: star4isaiah@yahoo.com

ABSTRACT
This study examined the bending, shearing, and deflection reliability of a reinforced concrete power transmission pole in Port Harcourt, Rivers State, under wind loading. The loading was completed in compliance with the Design Code of BS 8110: Part 3 (1997). Limit state functions were developed taking into account the reinforced concrete pole's failure in shear, deflection, and bending, respectively. With the use of MATLAB algorithms created using the First Order Reliability approach, the reliability indices corresponding to the limit states of bending, shearing, and deflection were determined. The deterministic design of the reinforced concrete pole, which was done in accordance with BS 8110: Part 3 (1197), provided the data for the reliability study. According to the results of the sensitivity analysis concerning the design parameters, the reliability indices generally increased as the concrete's characteristic strength, the concrete's characteristic strength of tension reinforcement, the area of tension reinforcement, the average pole diameter, the effective depth of reinforcement, and the ratio of reinforcements increased when the concrete pole's length and characteristic wind load increased, taking into account failure of the pole in bending, shearing, and deflection, respectively. In terms of reinforced concrete pole failure in bending, it is demonstrated that the pole is generally safe at reinforcement ratios of 1.65, 2.2, 2.75, and 3.0, which correspond to characteristic wind loads of 21.5 KN, 29 KN, 36.5 KN, and 40 KN, respectively. It is also generally safe at reinforcement ratios of 1.1, 1.65, 2.2, 2.75, and 3.0, which correspond to effective depths of 495 mm, 415 mm, 365 mm, 315 mm, and 300 mm, respectively. Taking into account the pole's failure in deflection, it is also shown that the pole is safe under typical wind loads of 26.5KN and 47KN, which correspond to pole lengths of 6m and 4.5m, respectively. Because the MATLAB-based computer algorithms are user-friendly, they may be used to estimate structural dependability.
Keywords: Reliability analysis, reinforced concrete transmission, power poles and wind load.

INTRODUCTION

Modern life would not be possible without electricity, since homes and businesses alike rely on a steady supply of this modern convenience. Integral to any stable electrical grid are the transmission and distribution networks. Now more than ever, meeting these demands requires an adequate transmission and distribution network infrastructure. Catastrophic occurrences could compromise human health and the dependability of the supply if this infrastructure is not built.

One material that can be shaped into many different sizes and shapes is reinforced concrete, which is used in architecture and construction. Conductors supported by concrete and wood poles are used to provide power in Nigeria, according to Quadri and Afoloyan (2017). The necessary voltage and

wattage determine the concrete pole's design. Since 33/11/0.415KV is often carried by overhead wires in Nigeria, both concrete and hardwood poles are acceptable for use. The loading concept, which takes into account the impact of loading on both the conductors and the materials used to make them, is the main basis for transmission pole structural designs.

As a consequence of the rural electrification project in Nigeria, the number of concrete poles used for electric power distribution has grown. In both rural and urban regions, efforts are being made to provide the necessary infrastructure and facilities for pole production to take place. Concrete poles can now support high voltage electrical transmission lines, thanks to recent technological advancements. Quadri and Afolayan (2017) state that reinforced concrete poles are very strong due to the fact that their bending moments exceed their shear pressures. In general, the compressive strength of concrete is strong and its tension is low. To make concrete members more resistant to tensile stresses, reinforcing bars are inserted into them.

As the number of homes and other structures requiring a continuous power supply continues to rise, there is a pressing societal demand for electric concrete poles. Like the human circulatory system, the electric power distribution network is connected to the producing station and the distribution system like the arteries in a person's body. Akin to capillaries, distribution networks link individual loads to transmission lines at substations that regulate and translate voltage. Energy is the lifeblood of civilization, and they are vital in delivering it to people everywhere. Electricity distribution lines consist of insulators, cross arms, distribution wires, and poles, as seen in Figure 1. Electric power distribution systems face several basic difficulties, including weather-related ones. These include wind, snow, and overtopping during seismic activity (Baghmisheh and Mahsuli, 2021; Ibrahim et al., 2017). Three 12-meter concrete poles tested under extreme weather conditions were examined by Zeynalian and Khorasgani (2018).

Environmental concerns, chemical attack, durability, high maintenance costs, and the desire for enhanced aesthetics have electric power distribution corporations searching for less costly alternatives to steel and wood poles (Salman and Li, 2016; Alkam and Lahmer, 2019). Therefore, concrete poles are impervious to wind, ice, heavy snow, marshy or wet soil, chemical pollution, polluted areas, where the deterioration rate of other pole materials might be unexpected, and other severe weather conditions. Concrete poles used for electric distribution might be subjected to severe weights during storms and vehicle accidents (Oyetola and Oritola, 2006; Phrommarat and Arromdee, 2019).

The reliability of a structure is related to how well it can estimate and anticipate the likelihood of limit-state violations at any particular time throughout its lifetime. By determining if the limit-state functions are exceeded, one may determine the likelihood of structural failure. The next stage, after identifying potential failure points, is to choose design solutions that will enhance structural dependability while decreasing failure risk (Choi et al., 2006). Finding essential parts and seeing whether adding more members will make the system more reliable by distributing the weight to nearby members are two examples of how structural reliability techniques are put into practice (Abejide, 2014).

The safety index and failure probability are the two key measures of reliability. This research use the First-Order Reliability Method (FORM) to calculate these measures, since they need approximations to limit-state functions. There should be almost no room for failure in built buildings, according to Nowak and Collins (2002). When dealing with these unknowns in reinforced concrete building processes, dependability analysis is a must. According to Thoft-Christensen and Baker (1982), reliability may be defined as the likelihood that, given a set of constraints, a structure will carry out its intended functions for a certain duration or reference period devoid of defects. Some kind of structural collapse is likely to occur. The employment of appropriate statistical and probability tools allows for the investigation of uncertainty around a structure's performance and structural safety.

Electrification of the National Local Government Headquarters and the whole rural electrification initiative are two examples of such development projects. During its installation, the concrete pole will provide a dependable system due to its design and the availability of systems for strength testing. The conductors and equipment supports in an electric overhead system need to be robust enough to endure the loads placed on them, and the conductors need to be able to sustain the weight of the equipment and the pressures applied to them. When you add the weight a pole has to support

to the horizontal loadings exerted at its top, you get the total amount of force acting on the pole. Conductors experience these later on due to wind pressure, unequal spans, offsets, and bends in the lines.

This research expands our understanding by offering solutions to the issues caused by the collapse of concrete electric transmission poles. These proposals have the potential to significantly alleviate these issues if they are put into action by the relevant authorities. Concrete poles are also required in locations where pollution and chemical contamination might speed up the decay of wooden poles (Anthony 1986). When the power needs of the poles outweigh those of wood poles and guying becomes a major challenge, concrete poles are the way to go. It is common practice to model concrete poles as cantilever beams with one end fixed when calculating their stresses. The pole is selected using these criteria in conjunction with the applicable safety considerations. On a pole, the following forces are at work:

As a whole, the cross arms, insulators, conductors, and associated gear contribute to the vertical loading.

Wind pressure on the pole and wires, known as horizontal loading.

Using the first-order dependability method, this work constructs and analyses a reinforced-concrete power transmission pole subjected to concentrated dead and wind loads. Bending, shearing, and deflection are the failure modes that are considered. For different values of the design parameters, the structural dependability is assessed using the MATLAB-based First Order reliability approach.

Improved and more equitable engineering design for reinforced concrete power transmission pole constructions in Nigeria and other developing nations is anticipated as a result of this study's ability to consider variable uncertainties and improve material optimization. Because transmission poles are vulnerable to so many different kinds of stresses—including wind, snow, ice, and earthquakes—our understanding of what causes them to fall is limited. On the other hand, these poles have more difficulties with wind loads because to the unexpected and highly geometric non-linear characteristics of wind turbulence. Wind speeds, which are influenced by both the mean and variable wind components, have an effect on transmission poles (Mustapha and Abejide, 2019). Major damage to poles and disruptions of the power supply have long been associated with natural disasters like earthquakes, along with the direct loss of property and lives caused by infrastructure damage. Industrial activities come to a standstill and significant financial losses are inflicted when the electricity supply goes out. How various parts of electrical transmission and distribution networks react to seismic waves determines how safe and reliable the system will be during an earthquake. it is essential to determine all the material-related elements in order to determine the load-bearing capabilities of a structure. Since the parameters mentioned uncertainty factors are essentially random and alter depending on the surrounding conditions, they asserted that a statistical approach might be used to calculate their mean and variation. Probabilistic evaluation is also a powerful tool for raising pole failure rates. Steel power distribution poles' structural reliability has not been thoroughly studied using probabilistic approaches. Given that all materials are susceptible to environmental degradation while in use, this represents a significant gap in the research. Because various pole materials degrade at different rates, it is challenging to create reliable prediction models that can be used to alter design strength components. Because of their unique strengths, durability, loading, and deterioration conditions, reinforced concrete power transmission poles display a great deal of variation compared to poles made of other materials (Afolayan and Abubakar, 2003).

Reinforced concrete energy transmission poles have a traditional design that prioritizes safety. This is why the resistance and load parameters are considered to be fixed, one-valued integers that do not take into account the design parameters' inherent variability. Most of the time, when deciding on safety considerations, experience and judgment are relied upon rather than a quantitative analysis of the associated uncertainties and failure likelihood. Offshore structural element design must make use of probabilistic ideas due to the unpredictability of most loads and material qualities.

Statement of Problem

Many reinforced concrete transmission poles in Nigeria have collapsed due to wind forces. Unfortunately, there has been a rise in the incidence of electric tapering concrete transmission pole failures, which has led to more frequent power outages, more traffic, and the tragic deaths of innocent people from electrocution. The electric pole fall in Port Harcourt's Tran-Amadi district in

2010 is a prime example; it killed dozens of people, destroyed millions of homes, and injured many more. Transmission poles made of reinforced concrete hold the wires that carry electricity above. Wind, shoddy construction, low-quality materials, and our outdated engineering design equation's partial safety factor all contributed to the destruction of many of these transmission poles in Nigeria. We can only over- or under-design structures or structural parts when we apply a partial safety factor in our typical engineering design equation, as real-world structural issues are stochastic rather than deterministic. It is not cost-effective and cannot guarantee structural safety. The inherent uncertainties in our design parameters have transformed reliability into a probability problem, which can only be resolved via the use of probability and statistics. Reliability is the ability of a facility or object to perform its function as expected within a certain time limit. On the other hand, it's all about failure and how it manifests. The dependability of reinforced concrete poles with respect to the limit states of bending, shearing, and deflection are investigated in this paper using a first-order reliability technique implemented in Matlab.

Aim and Objectives of the Study

The aim of this study is to carry out the reliability analysis of reinforced concrete pole used for power transmission in Rivers State subjected to wind loading.

The objectives are:

1. Carry out the code-based design of a reinforced concrete transmission pole structure under wing loading.
2. Develop the failure equations for a transmission pole structure under wind loading in bending, shear and deflection respectively.
3. Develop MATLAB programs to carry out the reliability analysis of reinforced concrete pole subjected to wind loading in Rivers State.
4. Carry out sensitivity analysis with respect to the design parameters in bending, shear and deflection respectively.

Empirical Explanation of the study

Electric or communications cables, transformers, streetlights, and other equipment rely on electrical poles to sustain their overhead transmission lines. Electric poles used to support transmission lines are known as transmission poles. Power poles made of wood or concrete often have tapered tips. Power outages, traffic congestion, and the tragic deaths of innocent people due to electrocution have all been exacerbated by the recent uptick in the collapse of electric energy distribution timber poles in Nigeria. When trying to estimate how long wood poles will last in operation, knowing how wind affects them is vital. Winds, poor building practices, and low-quality materials cause several reinforced wood power poles in Nigeria to collapse each year.

Utility pole breaks caused by wind are a common cause of service disruptions in metropolitan power distribution systems. For example, 113,640 customers lost electricity in 2018 when Hurricane Michael destroyed more than 79% of the poles in eight counties in North Florida. Nearly 121,000 people in Louisiana lost power as Hurricane Barry hit in July 2019. The storm brought down power wires from above. Power Transmission lines, commonly made of metallic wires, carry electrical current from power plants to substations, and then to residences, companies, and public services. Electrical conductors are usually made of metal alloys, such as copper, iron, aluminum, silver, or others.

Types of Electric Poles

Electric poles are categorized based on their production material, design structure, area of usage, and other characteristics which include

Steel, lattice steel, tower, rail, PCC, RCC, and wood are some of the many configurations that electric poles may take.

Wooden Electric Pole

The wooden electric pole is the most basic and inexpensive kind of infrastructure. Wooden electric poles are common in rural areas because they are easy to construct, cheap, and durable. Electric poles made of wood have a number of limitations, including a lower strength, a shorter height, and an inability to support long spans or droop.

PCC Electric Pole

An abbreviation for "plain cement concrete" is PCC. A standard height for this kind of pole is 7 to 8 meters. Use PCC poles for voltages of 230V, 440V, and 11KV. The durability of PCC poles is

superior to that of hardwood poles. Wooden poles are less costly than PCC poles, as one would expect. Primarily, the PCC pole is made of cement. This pole type can withstand more span and droop than its hardwood counterpart. Poles made of PCC are heavier than poles made of hardwood. A stray insulator-supported external conductor is suitable for these types of poles.

RCC Electric Pole

Concrete is the most widely used construction material in the world, second only in use to water. Cement, water, and aggregates are mixed in the right proportions to make it. In an ideal world, aggregates would make up 75% of concrete. This is because they play a pivotal role in the end product and must meet certain standards in order to produce durable, affordable concrete. The compressive, tensile, and flexural strengths of concrete remain its most essential features. These strengths evaluate the structural part's resistance to deformation. Research into the relationship between the chemical make-up of structural concrete and its mechanical properties is ongoing. According to Alhaji (2016), there seems to be a great deal of interest in concrete research, but this has not prevented instances of poor construction and structural collapse.

Wooden Electric Pole

Wood utility poles are basic structures that are used in electrical networks; wind is one of the major forces that might damage them. Their failure might lead to financial ramifications and severely affect dependability. The potential for a building to fall depends on the degree of demand and capacity uncertainty. A structure's load-bearing capacity is proportional to its shape and the characteristics of its materials. It is possible to treat the values of material properties as constants, although errors in these estimations are inevitable due to the materials' inherent properties. A fragility curve is one method that may be used to display the failure probability given a failure mechanism and a range of loads. Specifically, it's a way to assess how structural systems behave. Fragility curves are created for the structure and its individual parts. Argentine builders often use eucalyptus grand, a kind of wood commonly utilized for utility poles. The dynamic wind load is generated by taking a given Power Spectral Density Function (PSDF) and using the Spectral Representation Method (SRM) to extract the changing wind component.

Electricity Transmission Pole

In addition to supporting power lines and other public services and equipment like street lights, fiber optic cables, transformers, and electrical cables, electricity transmission poles—also called utility poles—are typically made of wood or reinforced concrete. Some people Telecom, electricity, hydro, and other utility poles are all part of the infrastructure. Electrical transmission poles constructed of reinforced concrete are shown in Plate 2.3, whereas those of wood are shown in Plate 2.2. Using electrical transmission poles allows for the secure storage of cables and electrical lines above ground, away from potential hazards such as automobiles and people, and with added insulation. Sub transmission lines transfer higher voltage power between substations, while distribution lines provide lower voltage energy to consumers. These conduits are used for both kinds of power lines.

Probabilistic Analysis Approach

Examining and predicting the possibility of limit state violation at any time over the structure's projected lifespan is an integral part of every structural element or member's reliability analysis. Structural reliability is a probabilistic analytic approach that focuses on performance measure violations. According to Opeyemi (2012). Natural disaster loads, such as those caused by wind, waves, storms, floods, earthquakes, etc., were known to be geographically and temporally unpredictable from the start.

The most fundamental problem with dependability is that there is only one load effect (S) that can be determined from an applied load (Q) and one resistance phenomena (R). Each of S and R is associated with a known probability density function, fS or fR. Structural collapse occurs when R is less than S. To get the failure probability, Eqn (2.4) is used.

$$pf = p(R \leq S) = P(R - S \leq 0) = P\ (RS \leq 1) \quad (2.4)$$

Equations (2.5) and (2.6), which are well-known rules for the addition (subtraction) of normal random variables, provide the mean and variance of the safety margin Z = R − S for normal random variables with few distributions of R and S.

$$\mu Z = \mu R - \mu S \quad (2.5)$$

$$\sigma 2Z = \sigma 2R + \sigma 2S \quad (2.6)$$

Equation (2.6) can be re-written as Equation (2.7).

$$pf = P\ (R - S \leq 0) = P\ (Z \leq 0) = \phi(0 - \mu Z \sigma Z) \quad (2.7)$$

Where ϕ is the standard normal distribution function (zero mean and unit variance)

$$pf = \mu R - \mu R - \mu S(\sigma 2S + \sigma 2R)12 = \phi(-\beta) \quad (2.8)$$

Where safety margin $\beta = (\mu Z\ \sigma Z)$ (2.9)

Failures of the Poles of Electrical Distribution System

Because of its dynamic nature, new concrete is a material whose qualities are always evolving. Reinforced concrete poles often fall due to corrosion of the steel reinforcing bars, since concrete is a plastic material rather than elastic.

Reinforced concrete poles use components like steel bars, timber beams, or fibers together with a wire framework to help shape the concrete. The concrete is strengthened and adequately supported by the reinforcement, which works in tandem with it. The concrete provides a sufficient barrier to slow the corrosion of the steel, making them a common component of modern buildings. An increase in conductor weight loads will be the consequence of rising stress on poles with a height profile that is greater than the average of surrounding poles. However, this effect is almost nonexistent on flat terrain.

Because the wind stresses the conductor, making it seem heavier than it really is, the tension will increase. Consequently, an increase in the resultant load will create an effective sag in an inclined direction with both horizontal and vertical concrete poles. Reports indicate that weather-related variables accounted for more than 80% of the reinforced concrete pole failures. Very Strenuous The wind, which encompasses tornadoes in all its forms as well as various gusts and microbursts associated with thunderstorms, is the primary element responsible for line failures. The fact that these poles have repeatedly collapsed due to high-velocity wind vibrations demonstrates that the engineer or technician responsible for their installation did not adequately account for the effects of wind. When making these poles, it's important to think about how the wind will affect them. An important step in the construction process could be caused by the wind load's effect on the reinforced concrete poles, however the force is always calculated after the installation is thought to be complete. Inadequately securing these poles to their bases is another potential cause of failure. The loads used in most codes of practice, standards, and design recommendations are based on large-scale wind storms that can be analytically treated. When it comes to wind damage on reinforced concrete poles buffeted by strong gusts, the "Gust loading Factor (GLF) method" has long been the go-to solution in most international standards and regulations. This scheme's design used a similar static wind loading, which is the mean wind force times the GLF. Although the

displacement responses are consistently approximated using the usual GLF method, it is possible that other response components are not.

Basic Concepts of Reliability Analysis

The reliability of an engineering design is the probability that it meets certain demands under certain conditions.

Mathematically, this can be represented as R>S.

This is mathematically expressed as:

$$\boldsymbol{Z = R - S} \quad (2.12)$$

Here Z is the performance function or limit state function of the foundation. This function differentiates the unsafe and safe zones with respect to R and S. This example has two stochastic variables R and S. This equation can be generalised as:

$$\boldsymbol{Z = (x)} \quad (2.13)$$

where g(x) constitutes the n basic variables x1, x2,.. xn of the performance function. The performance function owes it's name to the fact that it is a measure of the performance of any structure. Like any mathematical equation, the performance function could have three outcomes as follows:

$(x) > 0$: Safe region

$(x) = 0$: Limit state

$(x) < 0$: Failure region

2.13.5 Limit State Concept

On the x1-x2 plane, the contours are projections of the surface of fx (x1, x2). The probability density, or f (x), is the same at every point on the outlines.

This section identifies the benefits of FORM and provides some insight into the theory underpinning it, including the underlying mathematical equations. A viable substitute for the laborious Monte Carlo Analysis is FORM. Its mathematical complexity is compensated for by its precision with fewer calculations. Non-linear performance functions and associated non-normal variables may be handled with FORM. The Mean Value First order second moment method (MVFOSM) is another name for FORM. FORM uses the Taylor series approximation to linearize the performance function. It is a first-order approximation as a result. Only the variables' mean and standard deviation are used by FORM. The function for performance and limit state is provided by

$$\boldsymbol{Z = R - S} \quad (2.14)$$

As both R and S are assumed as normal random variables, Z can also be inferred as a random variable, that is $N(\mu R - \mu s, \sqrt{\sigma\frac{2}{R} + \sigma\frac{2}{S}})$.Then probability of failure can be defined as

$P_f = (Z < 0)$ (2.15)

$$P_f = \phi\left[\frac{0-(\mu_R-\mu_S)}{\sqrt{\sigma_R^2+\sigma_S^2}}\right] \quad (2.16)$$

$$P_f = 1 - \phi\left[\frac{(\mu_R-\mu_S)}{\sqrt{\sigma_R^2+\sigma_S^2}}\right] \quad (2.17)$$

ϕ is the CDF of the standard normal variate

Thus, the probability of failure is a function of the mean value of Z to its standard deviation.

$$\beta = \frac{\mu_Z}{\sigma_Z} = \frac{(\mu_R-\mu_S)}{\sqrt{\sigma_R^2+\sigma_S^2}} \quad (2.18)$$

The probability of failure can be expressed in terms of the safety index as follows.

$$p_f = \varphi(-\beta) = 1 - \varphi(\beta) \quad (2.19)$$

These variables are restricted to positive values. Hence log normally distribution is assumed.

The generalized formulation of the performance function can be written as:

Z =g (X) = g(X_1, X_2 … , X_n) (2.20)

X_1, X_2..X_n represents the random variables in the limit state function as mentioned before.

A Taylor series expansion of the limit state function about the mean gives

$$G = g(\mu_X) + \sum_{i=1}^{n} \frac{\partial g}{\partial X_i}\left(X_i - \mu_{x_i}\right) + \frac{1}{2}\sum_{i=1}^{n}\sum_{j-1}^{n} \frac{\partial^2 g}{\partial X_i \partial X_j}(X_i - \mu_{X_i})\left(X_j - \mu_{X_j}\right) + \cdots \quad (2.21)$$

The mean values are used to assess the gradient. Even though FORM is much less complex than is often believed, these computations make it less appealing for real-world applications. New FORM approaches use iterative restricted optimization algorithms that do not need assessment of the gradient in order to reduce the presumed mathematical complexity.

For linear terms, the Taylor series expansion is reduced to provide an approximate first order

The reduced expansion's mean and variance may be found using:

$\mu_z \approx (\mu_{X_1}, \mu_{X_2}, \ldots \ldots \mu_{X_n},)$ (2.22)

$$\sigma_z^2 \approx \sum_{i=1}^{n}\sum_{j=j}^{n} \frac{\partial g}{\partial X_i}\frac{\partial g}{\partial X_j} Cov(X_i, X_j) \quad (2.23)$$

($_{,j}$) is the covariance of X_i and X_j.

This explains the concept behind MVFOSM, which basically a Taylor series approximation or rather, linearization of the performance function at the mean values of the random variables.

2.13.6 Limitations of MVFOSM

1. Information about the variables' distribution is totally disregarded
2. For non-linear limit state functions, truncation errors resulting from linearization at the mean point.
3. Despite being technically identical, different equations produced different safety indices. Stated differently, the formulation of the limit state equation determines the safety indices.

The invariance issue was the term used to describe this.

Hasofer and Lind suggested a sophisticated First Order Reliability technique to solve the invariance issue.

2.13.7 Advanced First Order Reliability Method

As the name implies, this approach is a more sophisticated form of FORM that makes up for the dependability index's non-invariance in FORM. The variables are converted to a standardized space of normal variables using this procedure. Standard normal variables are known to have a standard deviation of one and a mean of zero. The purpose of this coordinate space translation is to facilitate the dependability index calculation. The reduction of a random variable X_i is:

$X'i = \frac{X_i - \mu_{X_i}}{\sigma_{X_i}}$ (i = 1,2,..,n) (2.24)

The probability density function of Xi', a random variable, has a unit standard deviation and zero mean. The limit state in the new space, the reduced coordinate space, is obtained by applying Equation 15 to the limit state equation. The appropriate limit state equation is produced by substituting the relevant reduced equation for each variable in the limit state equation. As shown in Figure 4, this is known as the transformation of the coordinate space from the original coordinates to the reduced coordinates. In the reduced coordinate system, g(X') = 0 is the limit state surface.

In this significantly smaller space, the dependability index is now specified. The smallest distance between the origin and the limit state surface is known as the Hasofer-Lind dependability index, or βHL. Therefore, there are two key components to determining this point: optimizing the distance to identify the ideal minimal distance point while keeping in mind that the point must be on the limit state surface. The design point (x*) is the minimal distance point on the limit state surface.

Hasofer – Lind index can be mathematically written as:

$\beta_{HL} = \sqrt{(x^*)^T}\sqrt{(x'*)T(x'*)}$ (2.25)

The design point represents the most probable point of failure - MPP

The transformation of the variables, R and S is as follows:

$$R' = \frac{R_i - \mu_S}{\sigma_R}, \quad S' = \frac{S_i - \mu_S}{\sigma_S} \tag{2.26}$$

Now the reduced equations of R and S are substituted into the limit state equation to obtain the new limit state surface in the standard space of coordinates.

$$Z = \sigma_R R' - \sigma_S S' + \mu_R - \mu_S \tag{2.27}$$

The reliability index is calculated using Equation 16. Reliability index can be estimated as:

$$\beta = \frac{\mu_Z}{\sigma_Z} = \frac{\mu_R - \mu_S}{\sqrt{\sigma_R^2 + \sigma_S^2}} \tag{2.28}$$

Probability of failure can be calculated from the reliability index.

$$P_f = \emptyset(-\beta_{HL}) \tag{2.29}$$

METHODOLOGY

Wind Load Estimation:

According to BS 6399: Part 2 (1997) Dynamic wind pressure is given as

$`q_w = 0.613 v_e^2$ **where**

$v_e = v_w k_1 k_2 k_3$

k_1, k_2, k_3 = risk factor 1.0**,;** terrain factor = 1.0 and topography factor = 1.0 respectively

According to Daramola and Oyetola (2005), the wind velocity in Port Harcourt, Rivers State is 5.6m/s. Therefore,

$$`q_w = 0.613*1.0*1.0*1.0*5.6^2 = 19.22 N/m^2$$

Wind Load on Pole

Force due to wind load on reinforced concrete pole =

$$F_{wp} = q_w * A_p = 19.22 * \frac{(0.250 + 0.15)}{2} * H_p$$

$$F_{wp} = 19.22 * \frac{(0.250 + 0.15)}{2} * 7.5 = 28.8N = 0.0288KN$$

A_p = projected area of reinforced concrete pole

H_p = length of reinforced concrete pole above the ground level respectively

Wind Load on Wires

Force due to wind load on wires =

$$F_{ww} = q_w * N_w * L_w * \phi_w = 19.22 * 3 * 50 * 0.00318 * 0.001 = 0.00917KN$$

N_w, L_w, ϕ_w =

Represents number of wires, Length of wire and diameter of wire respectively

Wind Load on Cross Arm and Insulator

Wind load on wires is transmitted to the cross arm and insulators. Therefore,

Force due to wind load on cross arm and insulator is the same as wind load on wires. Therefore,

$$F_{ci} = q_w * N_w * L_w * \phi_w = 19.22 * 3 * 50 * 0.00318 * 0.001 = 0.00917KN$$

N_w, L_w, ϕ_w =

Represents number of wires, Length of wire and diameter of wire respectively

Total wind load at the top level of the pole = wind load on pole + wind load on wire + wind load on cross arm and insulator. Therefore,

$$F_{tw} = F_{wp} + F_{ww} + F_{ci} \;= 0.0288 + 0.00917 + 0.00917 = 0.04714KN$$

Dead Load Estimation

Self-weight of Reinforced Concrete Pole

Density of concrete $= 24KN/m^3$

$$DL_p = \frac{\pi}{4}\left(\frac{\phi_{Top} + \phi_{Grd}}{2}\right)^2 * H_p * Density\ of\ Concrete$$

$$DL_p = \frac{\pi}{4}\left(\frac{0.25 + 0.15}{2}\right)^2 * 7.5 * 2400 * 10 * 0.001 = 5.66KN$$

ϕ_{Top}, ϕ_{Grd} = top and ground diameter of reinforced concrete pole respectively

Therefore, self weight of reinforced concrete pole = 5.66KN

Self-Weight of Aluminium Conductor

Self-weight of aluminium conductor = $0.86KN/m^2 * L_w * N_w * \phi_w$

Dead load of aluminium conductor = $0.86KN/m^2$ (Quadri and Afolayan, 2005; Mustafa and Abejide, 2006).

A_w = cross- sectional area of aluminium conductor

Self-weight of aluminium conductor

$= 0.86KN/m^2 * 50 * 3 * 0.00318 = 0.410KN$

Self-weight of Cross Arm and Insulator

Dead load on cross arm and insulator = $0.15KN/m^2$ (Quadri and Afolayan, 2005; Mustafa and Abejide, 2006).

Dead load on cross arm and insulator = $0.15KN/m^2 * L_w * N_w * \phi_w$

$$0.15KN/m^2 * 50 * 3 * 0.00318 = 0.0716KN$$

Therefore,

5.66 + 0.410 + 0.0716 = 6.14 KN is the total vertical load at the top of the reinforced concrete pole. Figure 3.1 depicts the reinforced concrete pole in this research that was exposed to concentrated dead and wind load at the top of the pole.

Development of the Performance Functions

The performance functions considered in the reliability study are derived based on the following structural failure modes:

i. Failure of reinforced concrete pole in bending
ii. Failure of reinforced concrete pole in shear
iii. Failure of reinforced concrete pole in deflection

Formulation of Limit State Functions

The limit state functions were derived in accordance with the design provisions of BS 8110: Part 1-3, 1997, for design of concrete structures.

Bending Limit State

The failure condition in bending is given by:

$$M_{ult} \le M_{app} \tag{3.1}$$

Therefore, the limit state function in bending is given by:

$$G(x) = M_{ult} - M_{app} \tag{3.2}$$

Where M_{ult} = ultimate moment of resistance of the beam, M_{app} = applied moment due to applied load on the beam

The maximum bending moment due to applied load is given by:

$$M_{app} = PH \quad (3.3)$$

Moment of resistance of a singly reinforced concrete beam based on concrete about the neutral axis of Figure 1 is given by:

$$M_{ult} = 0.156 f_{cu} b d^2 \quad (3.4)$$

Where f_{cu} = compressive strength of concrete, b = width of rectangular beam, d = effective depth of rectangular beam

Similarly,

The moment of resistance based on steel about the neutral axis of Figure 1 is given by:

$$M_{ult} = 0.95 f_y A_s Z \quad (3.5)$$

Where f_y = characteristic strength of steel, A_s = area of reinforcing bar, Z = lever arm distance

According to BS 8110, the lever arm distance z is given by:

$$Z = d - 0.45x \quad (3.6)$$

Substituting for z in Equation (3.5) using Equation (3.6) changes Equation (3.5) to:

$$M_{ult} = 0.95 f_y A_s (d - 0.45x) \quad (3.7)$$

Equation (3.7) can also be written as:

$$M_{ult} = 0.95 f_y A_s \, d \left(1 - 0.45 \frac{x}{d}\right) \quad (3.8)$$

According to BS 8110, for a singly reinforced concrete section,

$$\frac{x}{d} = 0.50 \quad (3.9)$$

Substituting for $\frac{x}{d}$ in Equation (3.8) using Equation changes Equation (3.8) to:

$$M_{ult} = 0.73625 f_y A_s \, d \quad (3.10)$$

Multiplying the right hand side of Equation (3.10) by $\frac{100bd}{100bd}$ changes Equation (3.10) to:

$$M_{ult} = 0.0073625 f_y A_s \, d * \frac{100bd}{bd} \quad (3.11)$$

$$\rho = \frac{100A_s}{bd} \quad (3.12)$$

Where ρ represents reinforcement ratio

Substituting for $\frac{100A_s}{bd}$ in Equation (3.11) changes Equation (3.11) to:

$$M_{ult} = 0.0073625 f_y \rho b d^2 \quad (3.13)$$

The point load at the top of the reinforced concrete pole consists of the point load due to dead load and wind load respectively.

According to BS 8110-1 (1997), the adverse load for the ultimate limit state is given by:

$$P = 1.4G_k + 1.4Q_k \quad (3.14)$$

Let:

$$\alpha = \frac{G_k}{Q_k} \quad (3.15)$$

Equation (3.14) therefore becomes:

$$P = (\alpha + 1)1.4Q_k \quad (3.16)$$

Applying Equation (3.16), Equation (3.3) becomes:

$$M_{app} = (\alpha + 1)1.4Q_k H_p \quad (3.17)$$

Applying Equation (3.13) and Equation (3.17), the limit state function in bending based on steel capacity is given by:

$$G(x) = 0.0073625 f_y \rho b d^2 - (\alpha + 1)1.4Q_k H_p \quad (3.18)$$

Also, applying Equation (3.4) and Equation (3.17), the limit state function in bending based on concrete capacity is given by:

$$G(x) = 0.156 f_{cu} b d^2 - (\alpha + 1)1.4Q_k H_p \quad (3.19)$$

Similarly, applying Equation (3.7) and Equation (3.17), the limit state function in bending based on steel capacity is given by:

$$G(x) = 0.73625 f_y A_s\ d - (\alpha + 1)1.4Q_k H_p \quad (3.20)$$

Shear Limit State

The shear resistance of concrete is given by:

$$V_c = \upsilon_C b d \quad (3.21)$$

The shear resistance of link is given by:

$$V_{link} = \frac{A_{sv}}{S_v} 0.87 f_y d \quad (3.22)$$

Therefore, the total resistance in shear offered by concrete and link reinforcement Is given by:

$$V_c = \upsilon_C b d + \frac{A_{sv}}{S_v} 0.87 f_y d \quad (3.23)$$

From equation (3.17), the maximum shear force acting on the pole is given by:

$$V_{\max} = P \quad (3.24)$$

Applying Equation (3.16), Equation (3.24) becomes:

$$V_{\max} = (\alpha + 1)1.4Q_k \quad (3.25)$$

According to BS 8110 (1997), the design concrete shear stress, v_c is given by:

$$v_c = \frac{0.79}{\gamma}\left(\frac{100A_s}{bd}\right)^{\frac{1}{3}} * \left(\frac{400}{d}\right)^{\frac{1}{4}} * \left(\frac{fcu}{25}\right)^{0.33} \quad (3.26)$$

Applying Equation (3.23) and Equation (3.25), the limit state function in shear becomes:

$$G(x) = \frac{A_{sv}}{S_v} 0.95 f_y d + \upsilon_C b d - (\alpha + 1)1.4Q_k \quad (3.27)$$

Deflection Limit State

The design constraint in deflection is given by:

$$\delta_{all} = \frac{L}{250} \quad (3.28)$$

From basic strength of materials, for a cantilever beam carrying a point load at the top, the maximum deflection is given by:

$$\delta_{\max} = \frac{PL^3}{3EI} \tag{3.29}$$

Applying Equation (3.28) and Equation (3.29), the limit state function in deflection is given by:

$$G = \frac{L}{250} - \frac{PL^3}{3EI} \tag{3.30}$$

Applying Equation (3.25), Equation (3.30) changes to:

$$G = \frac{L}{250} - \frac{(\alpha + 1)1.4Q_k L^3}{3EI} \tag{3.31}$$

First Order Reliability Method

The First Order Reliability method is an approximate method of computing the probability failure of a system with random variables was used for reliability estimation.

The vector of random variables, are the basic variables having joint probability function given by:

$$x = (x_1, x_2, ..., x_n) \tag{3.32}$$

Regarding the fundamental variables, the First Order Reliability Method is continuous and differentiable. This indicates the existence of the probability density. The failure function of a structure that corresponds to a certain limit state is often a function of the fundamental variables and denotes the structure's safe state, limit state surface, and failure state.

The random discrepancy between a structure's resistance and load effects is known as the failure function. The performance function for n-dimensional random variables is as follows:

$$G(X) = G(X_1, X_2, X_3, ..., X_n) = R(X) - S(X) \tag{3.33}$$

Where $X_1, X_2, X_3, ..., X_n$ the basic are design variables; $R(X)$ and $S(X)$ is structural resistance and load effect.

From Equation (3.4), the limit state equation is given by:

$$G(X) = G(X_1, X_2, X_3, ..., X_n) = 0 \tag{3.34}$$

Non-normal random variables x_i are transformed into independent normal variables using the transformation:

$$Z = \frac{X_i - \mu_{xi}}{\sigma_{xi}}, \quad (i = 1, 2, ..., n) \tag{3.35}$$

Using equation (3.35), the limit state equation for n transformed variates is given by:

$$G(\sigma_{x1} * Z_1 + \mu_{x1}, \sigma_{x2} * Z_2 + \mu_{x2}, \sigma_{x3} * Z_3 + \mu_{x3}, ..., \sigma_{xn} * Z_n + \mu_{xn}) = 0 \tag{3.36}$$

The vector of the design point on the failure surface $G(X_i^*) = 0$ to the origin of the design in z space is given by:

$$Z^* = (Z_1^*, Z_2^*, Z_3^*, Z_n^*) \tag{3.37}$$

The structural reliability index β is the minimum from the most probable failure point on the failure surface $G(X_i^*) = 0$ to the origin of the design variable space. This minimum distance is given by:

$$\|D\| = \beta = \sqrt{(Z_1^{*2} + Z_2^{*2} + Z_3^{*2} + ... + Z_n^{*2})} \tag{3.38}$$

The design point $Z^* = \left(Z_1^*,\ Z_2^*,\ Z_3^*,\ Z_n^*\ \right)$ is determined by minimizing the Equation (3.38) subject to Equation (3.34).
The First order approximation to probability of failure is given by:

$$P_f = P(G(X) \leq 0 = \phi(-\beta) \qquad (3.39)$$

Where β = reliability index which represents the minimum distance between the origin and the failure surface

Transformation of Non-Normal Variables

All non-normal variables in the performance functions are first transformed into equivalent normally distributed variables.

According to Ranganthan (1999), the equivalent normal variables are made equal at the design point, $x = \left(x_1^*, x_{2,}^* x_3^*, ..., x_n^*\right)$ on the failure surface.

Each statistically independent non-normal variable is equated with an equivalent normal variable at the design point to yield:

$$\Phi\left(\frac{x_i^* - \mu_{xi}^N}{\sigma_{xi}^N}\right) = Fx_i(x_i^*) \qquad (3.40)$$

where $\Phi(\cdot)$ = cumulative distribution function of the standard normal variable at the design point; μ_{xi}^N, σ_{xi}^N represents the mean and standard deviation of the equivalent normal variable at the design point respectively, $Fx_i(x_i^*)$ = cumulative distribution function of the original non-normal variables.

The mean of the equivalent normal variable at the design point is given by:

$$\mu_{xi}^N = x_i^* - \Phi^{-1}\left[Fx_i\left(x_i^*\right)\right]\sigma_{xi}^N \qquad (3.41)$$

Equating the probability distribution functions of the original variable and the equivalent normal variable at the design point yields:

$$\frac{\phi}{\sigma_{xi}^N}\left(\frac{x_i^* - \mu_{xi}^N}{\sigma_{xi}^N}\right) = fx_i(x_i^*) \qquad (3.42)$$

Where $\phi(\cdot)$ and $fx_i(x_i^*)$ = probability distribution function of the equivalent standard normal and the original non-normal random variable respectively.

$$\Phi^{-1}\left[Fx_i\left(x_i^*\right)\right]\sigma_{xi}^N = x_i^* - \mu_{xi}^N \qquad (3.43)$$

Applying Equations (3.40), (3.41), (3.42) and (3.43), the standard deviation of the equivalent normal variables is given by:

$$\sigma_{xi}^{N} = \phi \frac{\left(\Phi^{-1}\left[F_{xi}\left(x_i^*\right)\right]\right)}{fx_i\left(x_i^*\right)} \qquad (3.44$$

A Reinforced Concrete Rectangular Transmission Pole for Reliability Study

Figure 3.1 depicts a 7.5-meter-long, rectangular, reinforced concrete transmission pole under concentrated dead and evenly distributed wind load, as determined by the design guidelines of BS 8110: part 1-3, 1997 and BS 5400 (1997), respectively.

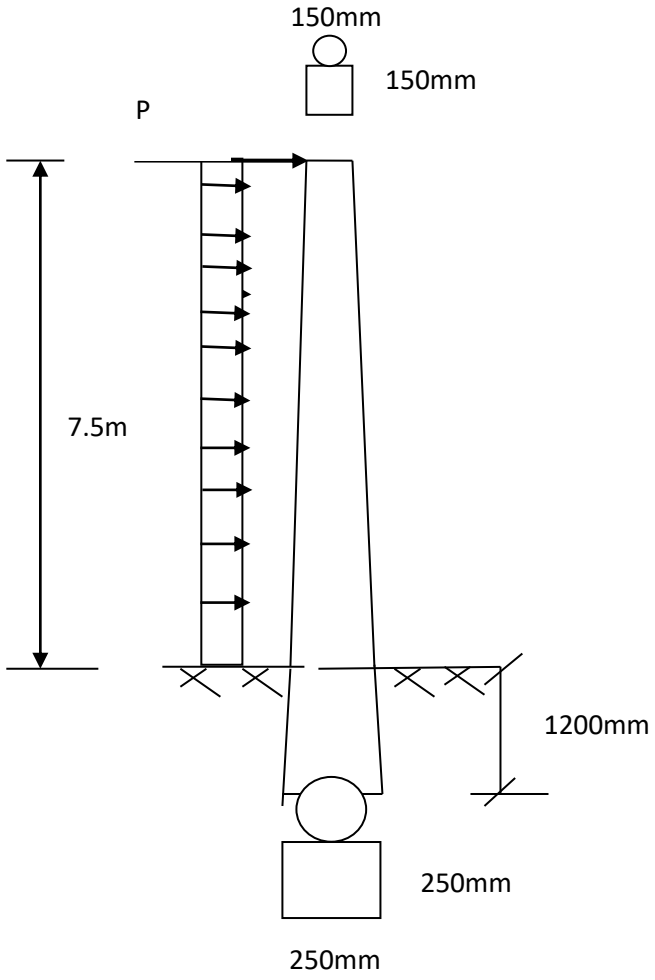

Plate 3.1: Reinforced Concrete Pole under Dead and Wind load

RESULTS

The statistics of the basic variables are presented in Table 1. The uncertainty corresponding to all the random variables are obtained based on information obtained from literature on the design variables.

Table 1: Statistics of the Basic Random Variables

Variable	Mean	Standard Deviation	Variation Coefficient	Probability Density Function
Area of tension steel, A_s	905 mm^2	13.575 mm^2	0.015	Normal
Effective depth, d	219 mm	8.76 mm	0.04	Normal
Beam span, L	7500 mm	375 mm	0.05	Normal
Moment of Inertia, I	1.94*10^8mm^4	9700000mm^4	0.05	Normal
Modulus of Elasticity, E	26000N/mm^2	780N/mm^2	0.03	Normal
Yield strength of steel, f_y	460 N/mm^2	69 N/mm^2	0.15	Normal
Wind Load, Q_k	47.14N	16.5N	0.35	Gamma
Diameter of pole, b	250 mm	10 mm	0.04	Normal
Concrete strength, f_{cu}	30 N/mm^2	5.4 N/mm^2	0.18	Normal
Steel ratio, ρ	Vary	Vary	Vary	Deterministic
Area of link reinforcement, A_{sv}	101 mm^2	1.5165 mm^2	0.015	Normal
Spacing of link reinforcement, S_v	150 mm	6 mm	0.04	Normal
Yield strength of link reinforcement, f_{yv}	250 N/mm^2	12.5 N/mm^2	0.05	Normal
Area per spacing of link, A_{sv}/S_v	0.673	-	-	Fixed
Dead Load , P	5600	290	0.05	Normal
α	130.25	Deterministic	Deterministic	Deterministic

RESULTS

The results of the reliability analysis of the reinforced concrete transmission pole in bending, shear and deflection using First Order Reliability method coded in MATLAB language are presented in Figure 1 to Figure 18 respectively.

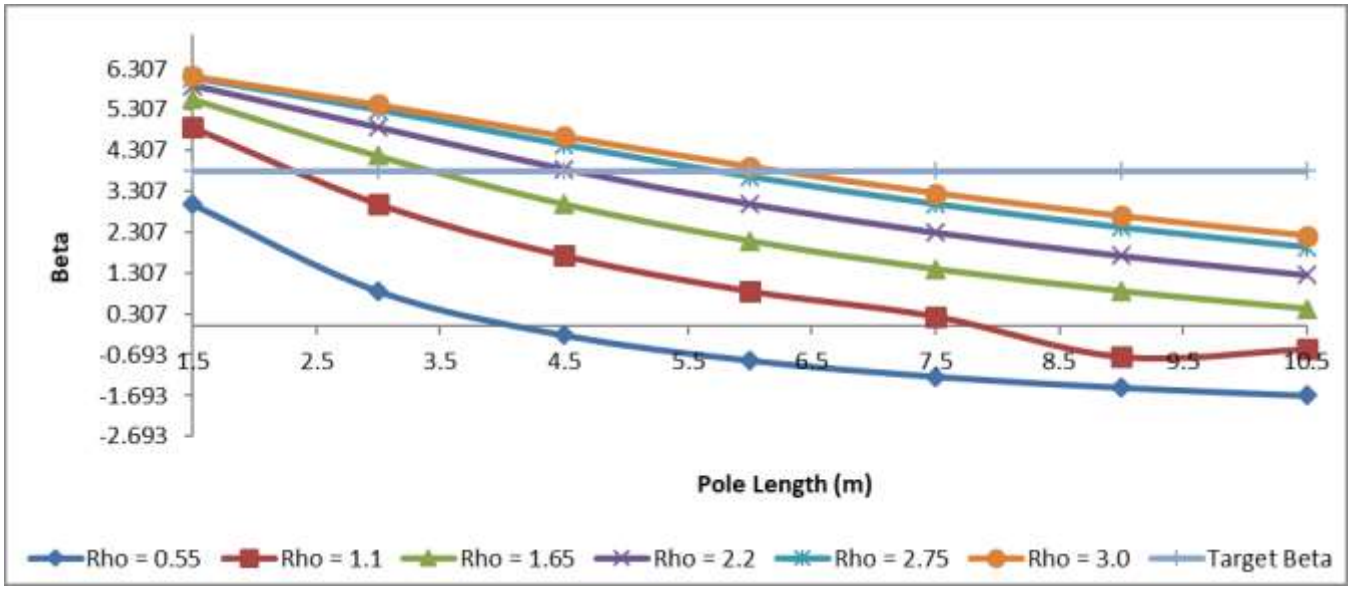

Figure 1: Relationship between Reliability Indices and Length of Pole at varying Reinforcement Ratio (Bending Criterion)

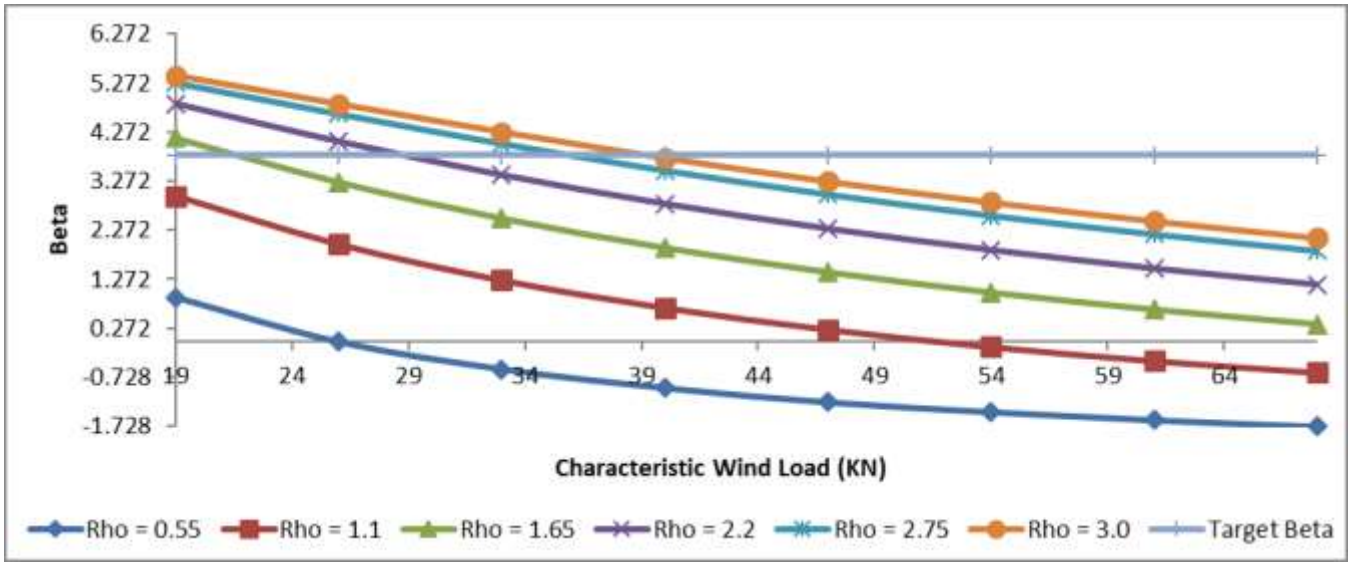

Figure 2: Relationship between Reliability Indices and Characteristic Wind Load at varying Reinforcement Ratio (Bending Criterion)

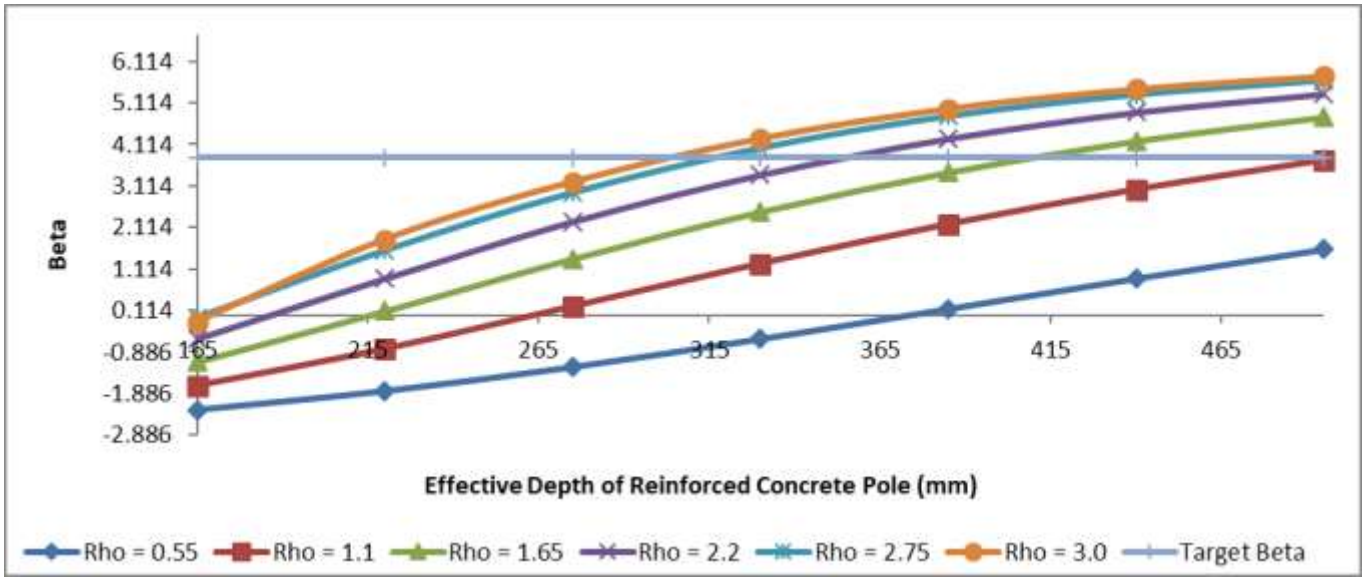

Figure 3: Relationship between Reliability Indices and Effective Depth at varying Reinforcement Ratio (Bending Criterion

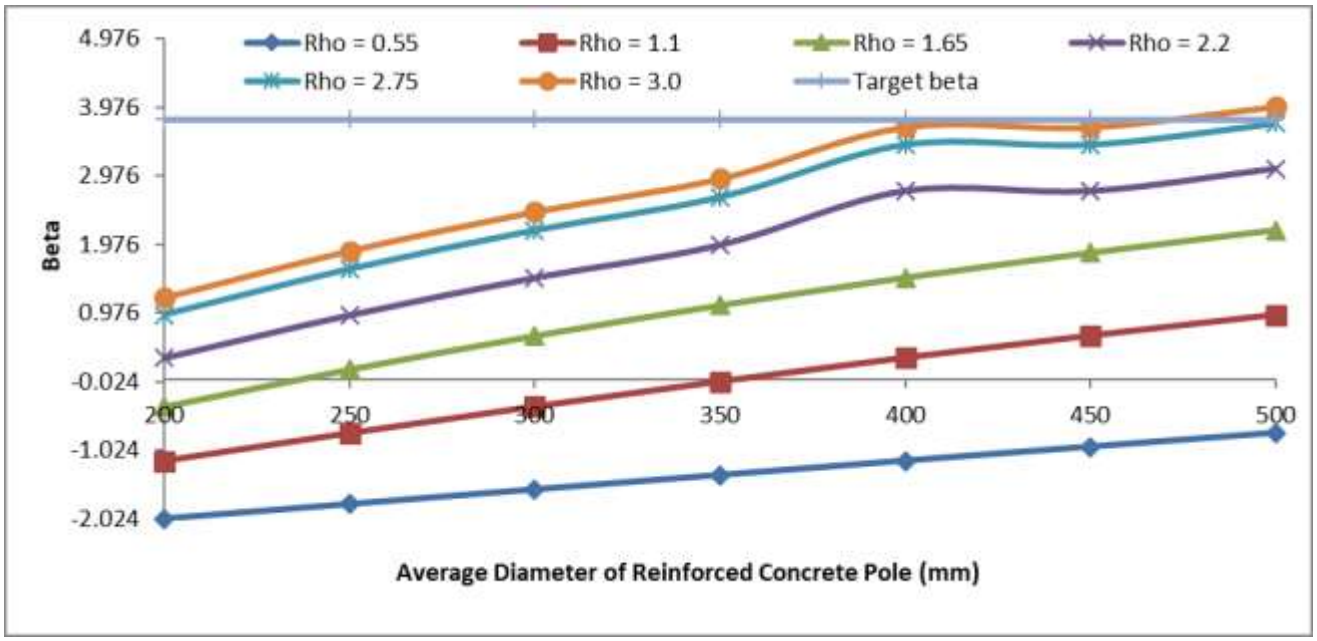

Figure 4: Relationship between Reliability Indices and Average Diameter of Pole at varying Reinforcement Ratio (Bending Criterion)

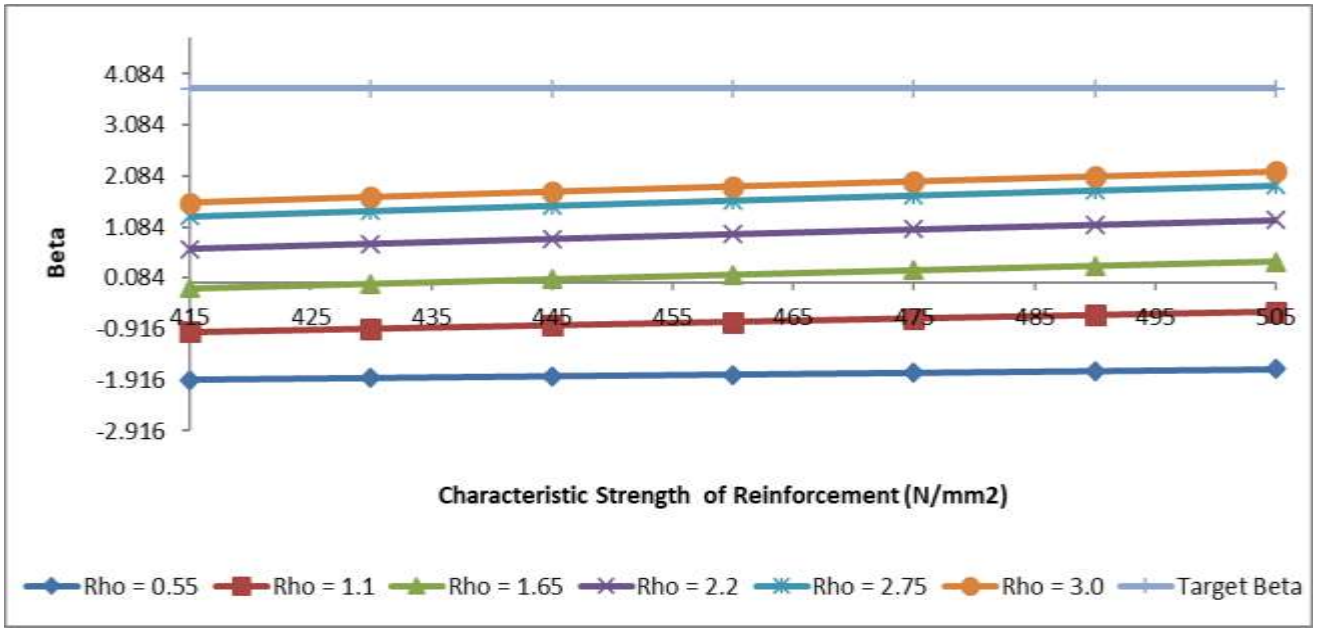

Figure 5: Relationship between Reliability Indices and Characteristic Strength of Reinforcement at varying Reinforcement Ratio (Bending Criterion)

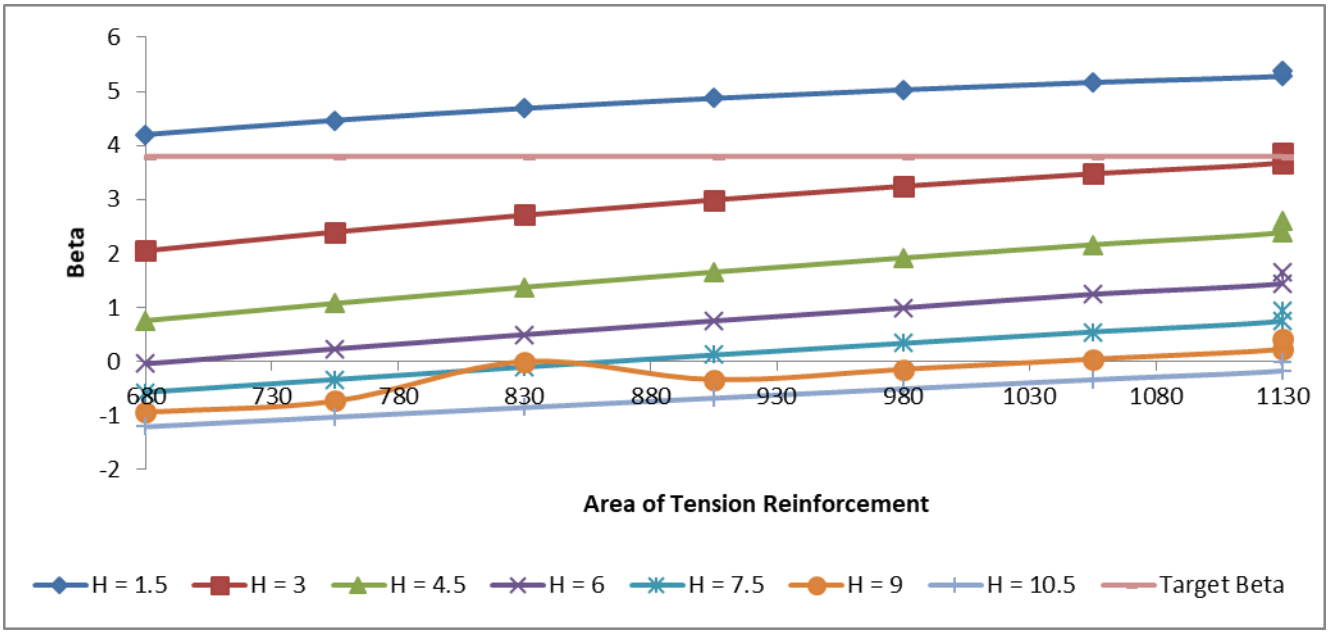

Figure 6: Relationship between Reliability Indices and Area of Tension Reinforcement at varying Length of Reinforced Concrete Pole (Bending Criterion)

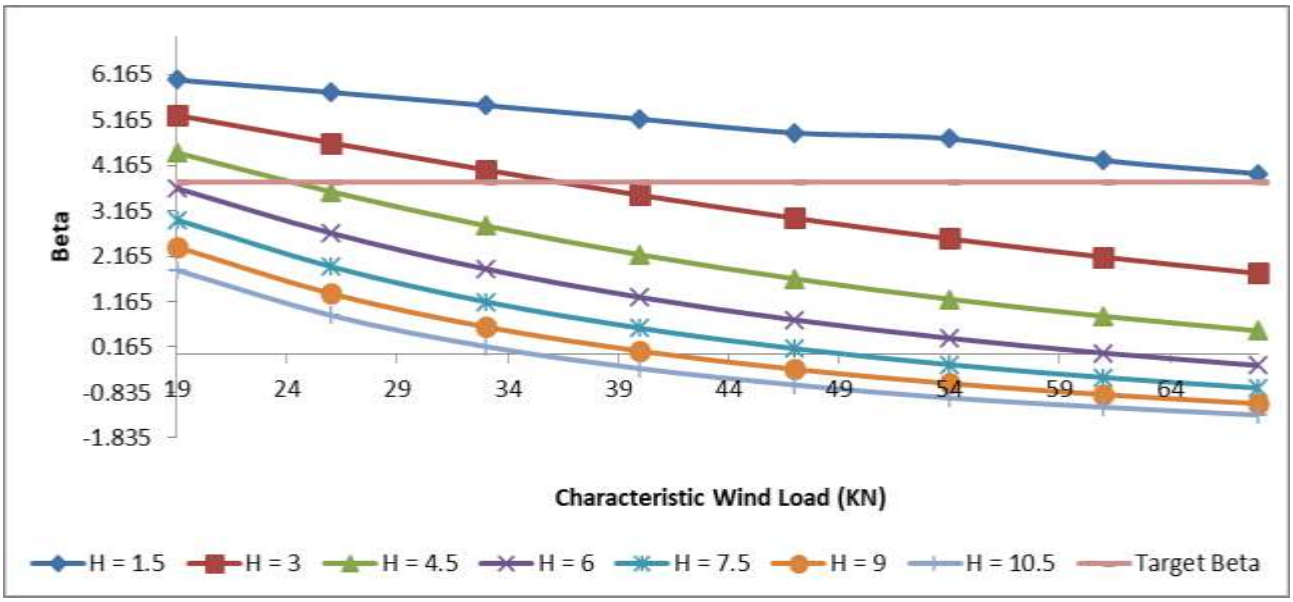

Figure 7: Relationship between Reliability Indices and Characteristic Wind Load at varying Length of Reinforced Concrete Pole (Bending Criterion)

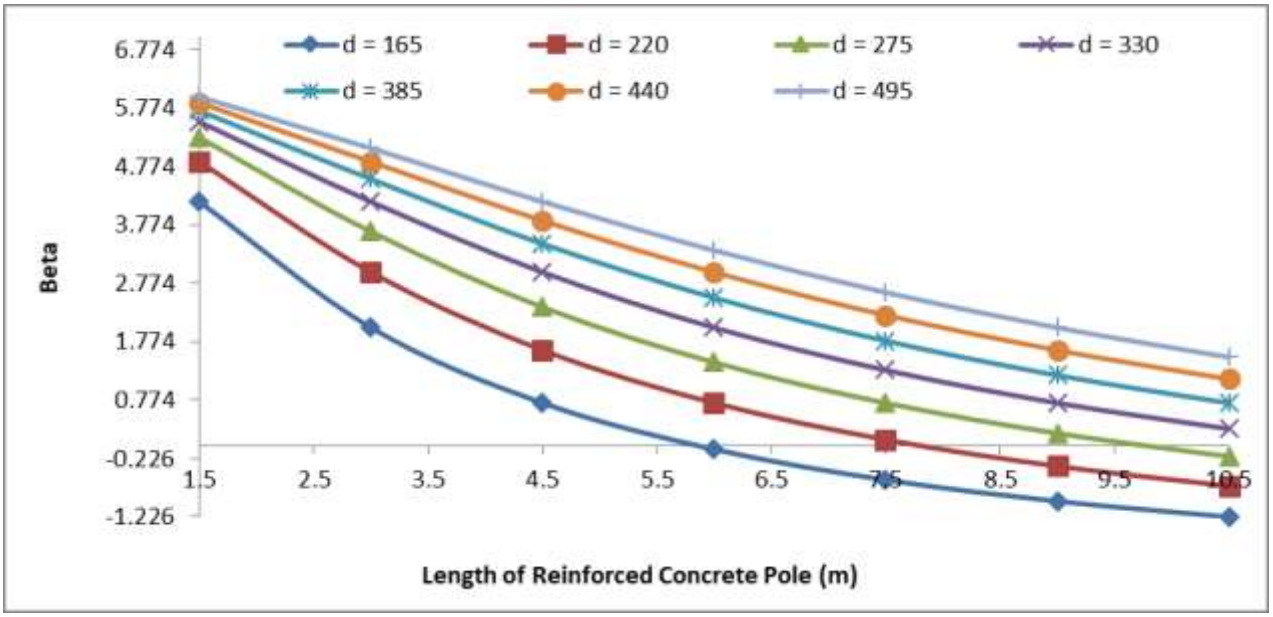

Figure 8: Relationship between Reliability Indices and Height of Pole at varying Effective Depth of Pole (Bending Criterion)

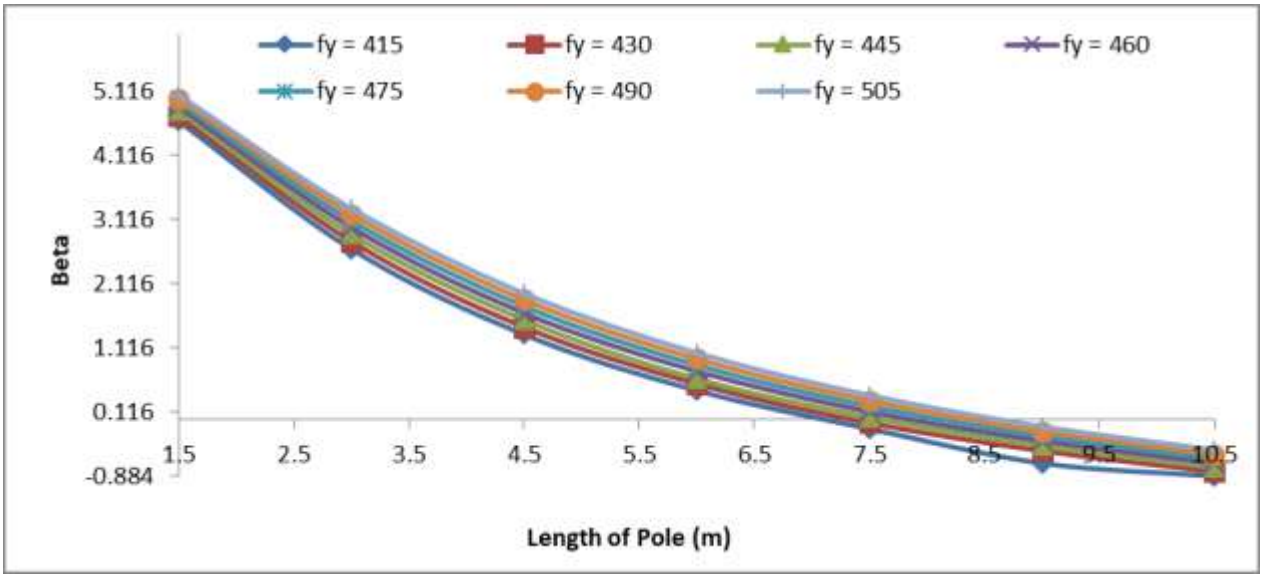

Figure 9: Relationship between Reliability Indices and Length of Pole at varying Characteristic Strength of Reinforcement (Bending Criterion)

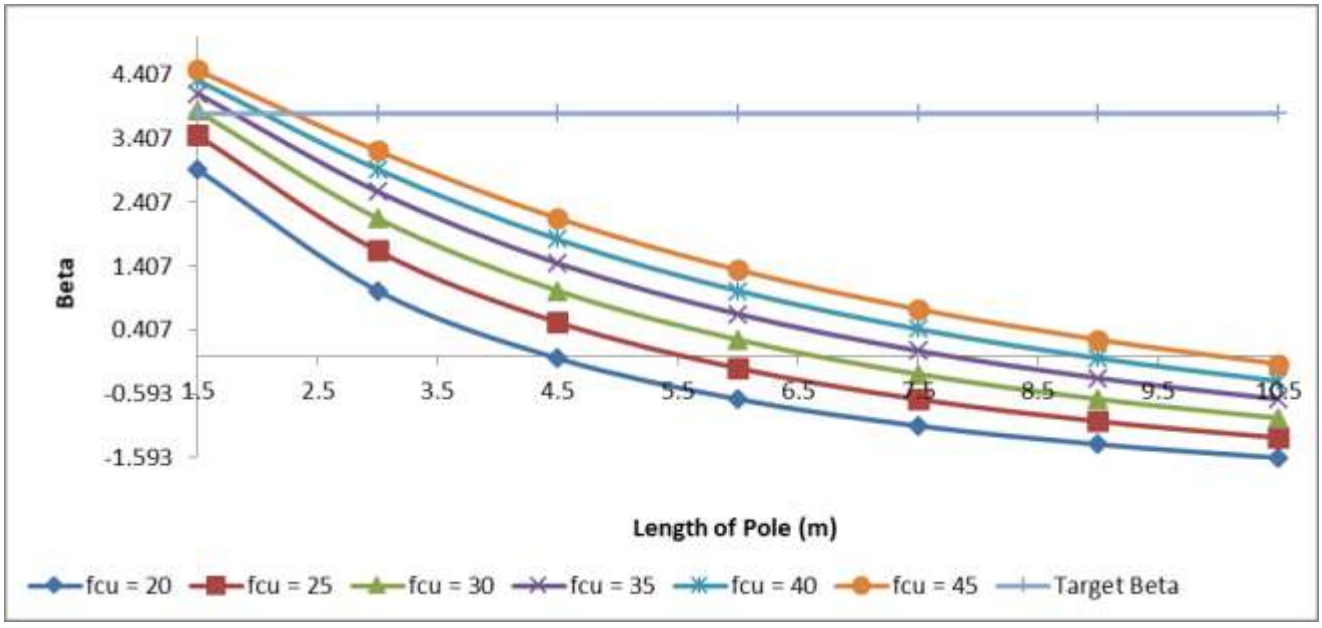

Figure 10: Relationship between Reliability Indices and Length of Pole at varying Characteristic Strength of Concrete (Bending Criterion)

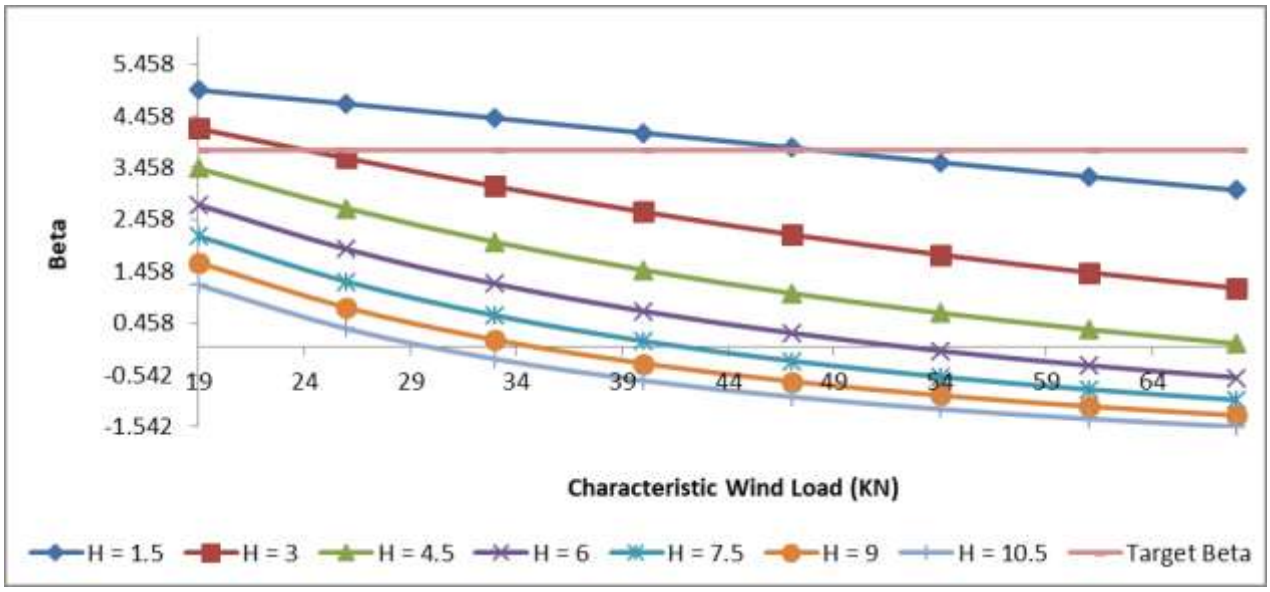

Figure 11: Relationship between Reliability Indices and Length of Pole at varying Characteristic Strength of Concrete (Bending Criterion)

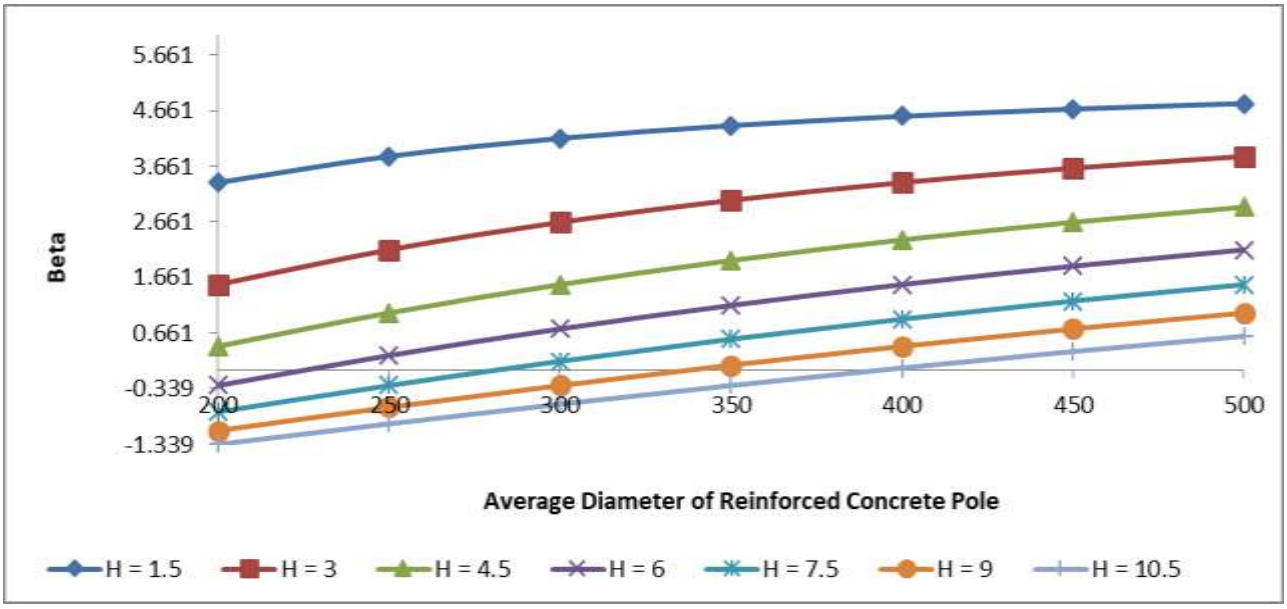

Figure 12: Relationship between Reliability Indices and Average Diameter of Reinforced Concrete Pole at varying Length of Pole (Bending Criterion)

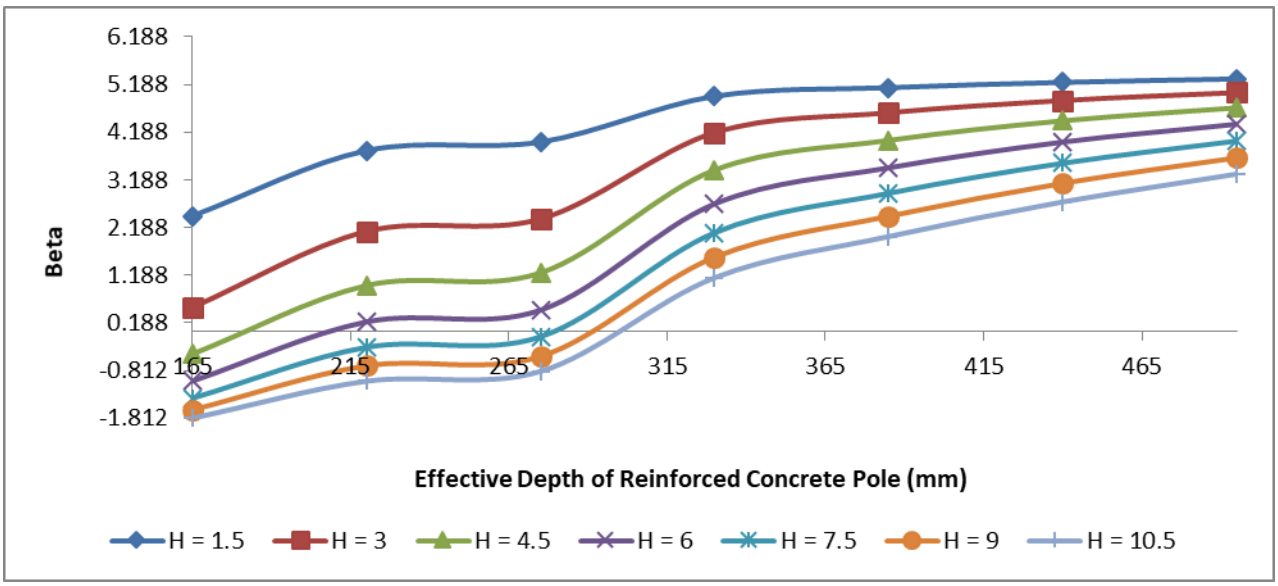

Figure 13: Relationship between Reliability Indices and Effective Depth of Reinforced Concrete Pole at varying Length of Pole (Bending Criterion)

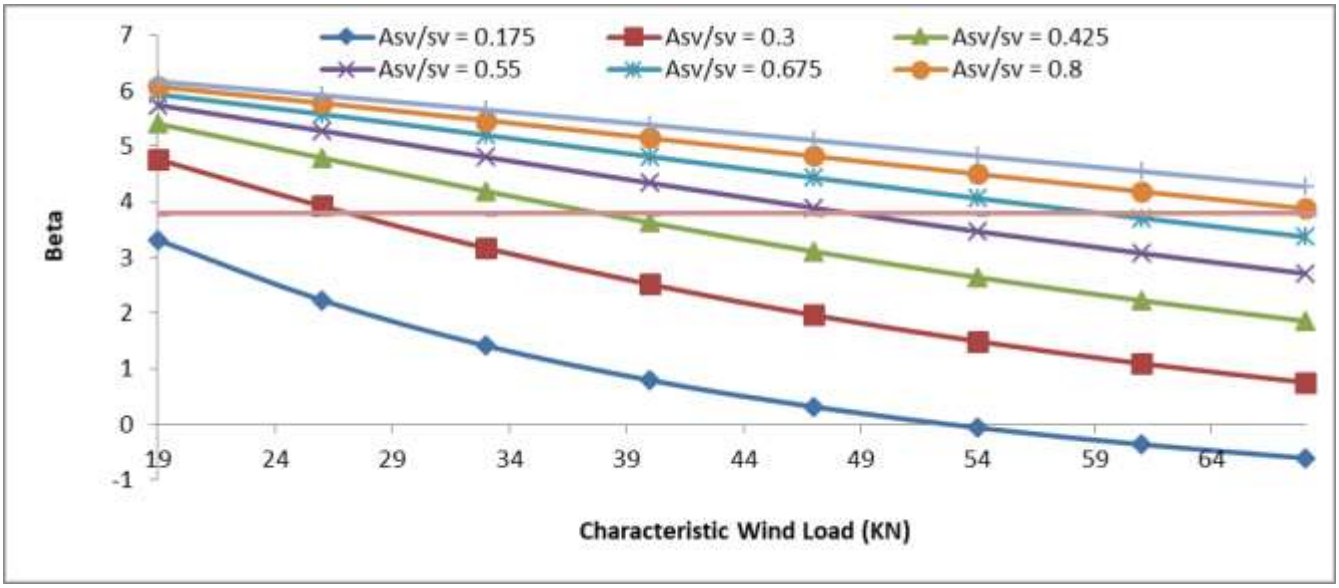

Figure 14: Relationship between Reliability Indices and Characteristic Wind Load at varying Area/Spacing of Link Reinforcement (Shear Criterion)

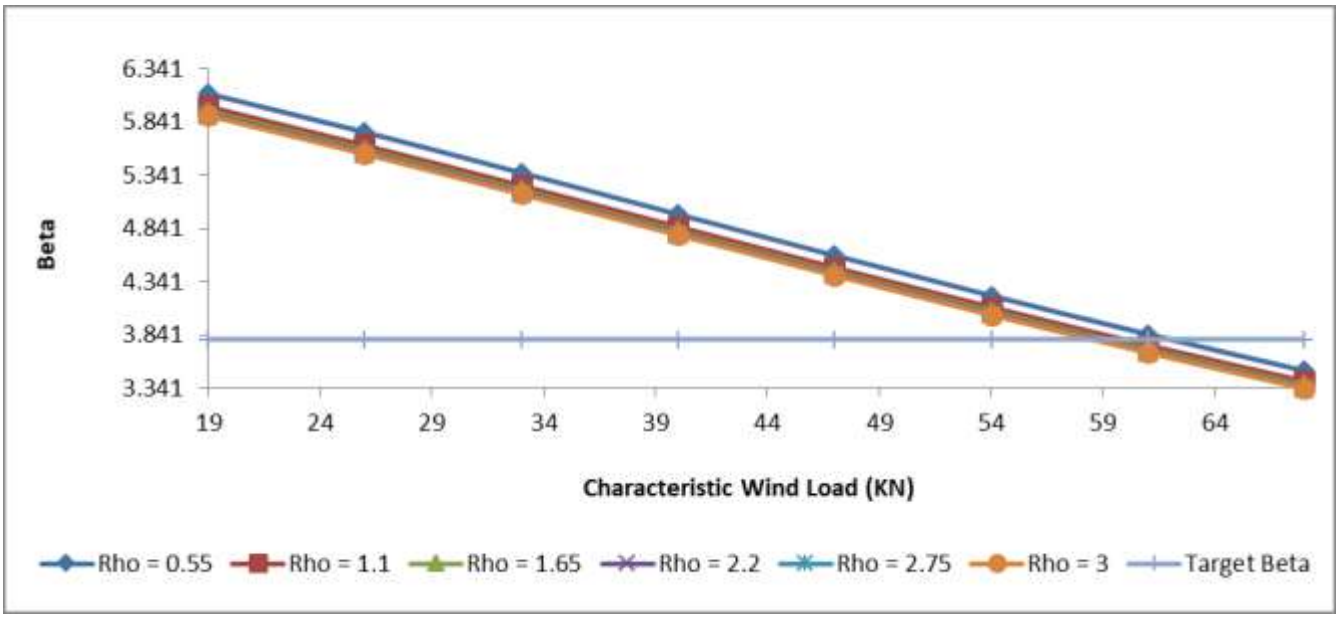

Figure 15: Relationship between Reliability Indices and Characteristic Wind Load at varying Reinforcement Ratio (Shear Criterion)

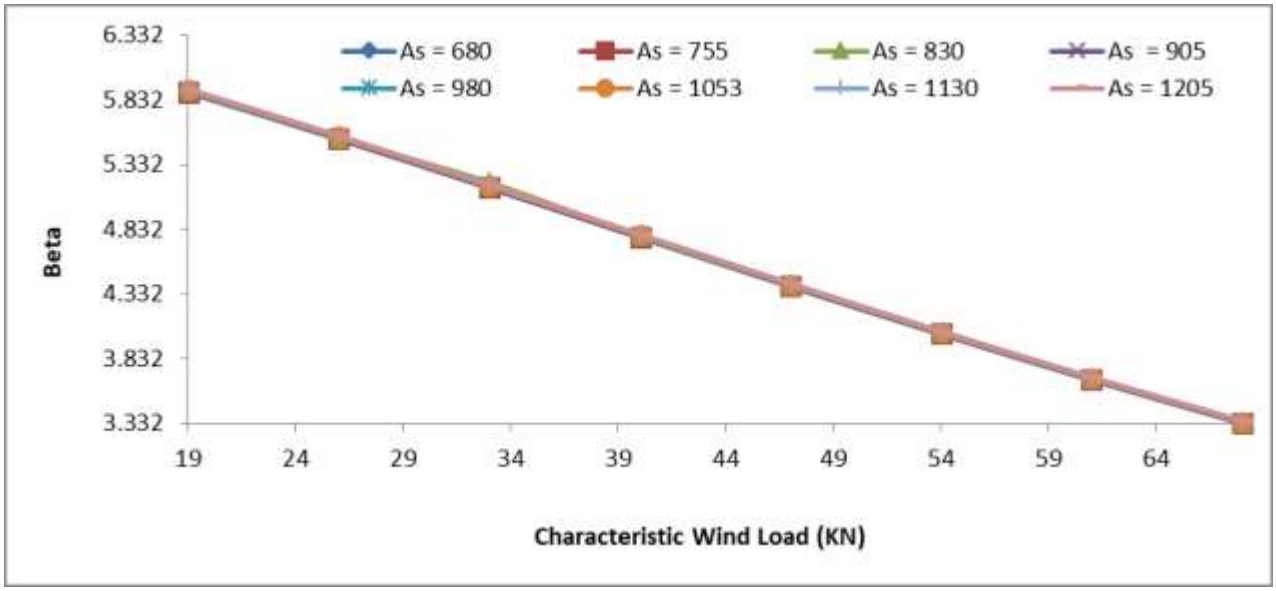

Figure 16: Relationship between Reliability Indices and Characteristic Wind Load at varying Area of Steel Reinforcement (Shear Criterion)

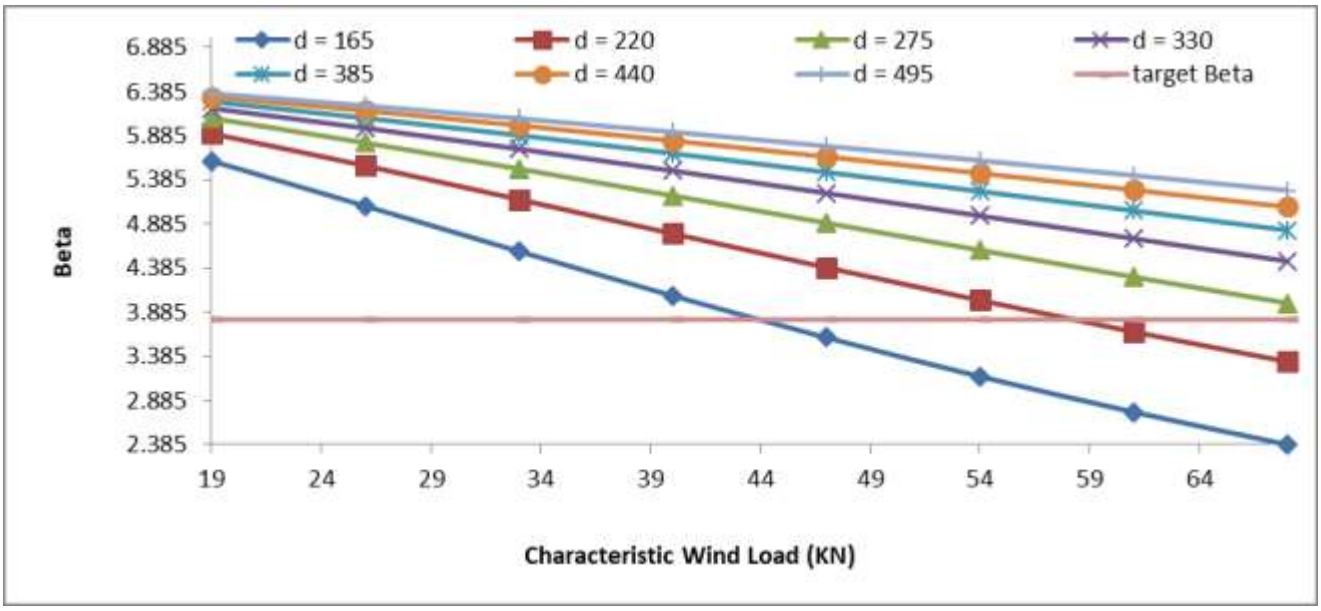

Figure 17: Relationship between Reliability Indices and Characteristic Wind Load at varying Effective Depth (Shear Criterion)

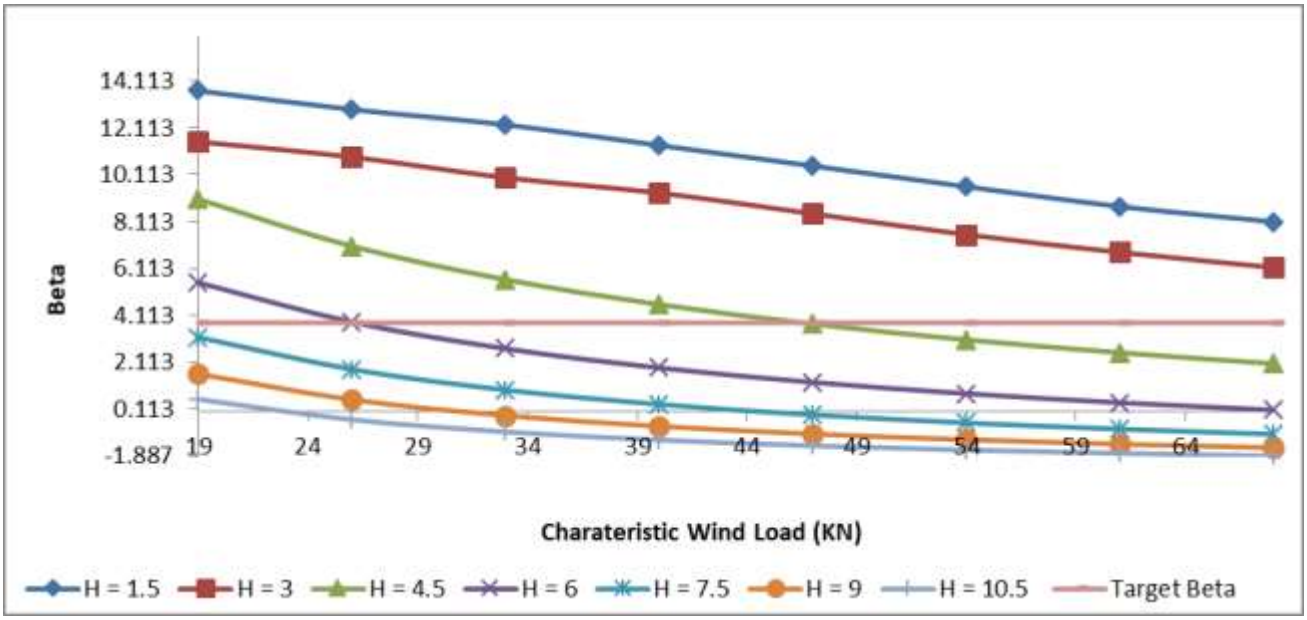

Figure 18: Relationship between Reliability Indices and Characteristic Wind Load at varying Length of Pole (Deflection Criterion)

DISCUSSION OF FINDINGS

A MATLAB program built on the First Order reliability approach was used to generate the safety indices for the limit states of bending, shear, and deflection taken into consideration in this work. The results of the dependability indices against different values of the reinforced concrete pole's design parameters, taking into account the concrete's capacity in tension and compression, shear, and deflection, respectively, are shown in Figures 1 to 18. Figure 1 illustrates how dependability indices rise with an increase in reinforcement ratio and fall with an increase in pole length. This pattern is consistent with the findings of Quadri and Afolayan (2017). Pole dependability indices decrease in proportion to an increase in pole length. This may be explained by the fact that as pole length increases, the applied bending moment increases as well. It may be possible to link the rise in reliability indices with an increase in the reinforcement ratio to an increase in the tension reinforcement value, which in turn raises the pole's dependability. Figure 1 shows that the suggested goal dependability index of 3.8 is met at reinforcement ratios of 1.65, 2.2, 2.75, and 3.0, which correspond to pole lengths of 3.5, 4.5, 6m, and 6.5m (EN, 1990). The connection between the typical wind load and the indicated reliability indices at different reinforcement ratio values is shown in Figure 2. Additionally, as shown in Figure 2, the reliability indices decline as the typical wind load and reinforcement ratio rise, respectively. As the characteristic wind load on the pole increases, the bending moment on the pole increases as well, which is why reliability indices decrease as the reinforcement ratio increases. Conversely, when the reinforcement ratio increases, the values of the tension reinforcement also increase, increasing pole reliability. This pattern is consistent with the findings of Quadri and Afolayan (2017). Figure 2 shows that the pole is safe at reinforcement ratios of 1.65, 2.2, 2.75, and 3.0, which correspond to two-and-a-half, 29, 36.5, and 40 KN of typical wind load, respectively. As can be shown, the typical wind load should not exceed 26.5KN and 47KN for reinforcement ratio values of 0.55 and 1.1, respectively, as doing so results in negative dependability indices. Negative dependability index readings indicate that the construction is completely unsafe, claims Abejide (2014).

The link between the effective depth of the reinforced concrete pole section and the inferred reliability indices at different reinforcement ratio values while taking the concrete capacity under stress into account is shown in Figure 3. Figure 3 further shows that the dependability indices rise in proportion to increases in the effective depth reinforcement ratio. It's possible that an increase in moment capacity leads to a proportional improvement in the reliability of reinforced concrete poles, which explains why reliability indices rise as effective depth and reinforcement ratio increase. This pattern is consistent with the findings of Quadri and Afolayan (2017). The reinforced concrete pole is safe because it meets the necessary target dependability index of 3.8 (EN, 1990). Figure 3 shows that the pole is safe for reinforcement ratios of 1.1, 1.65, 2.2, 2.75, and 3.0, which correspond to effective depths of 495 mm, 415 mm, 365 mm, 315 mm, and 300 mm.

The link between the average diameter of the reinforced concrete pole section and the indicated reliability indices at different reinforcement ratio values while taking the concrete capacity under stress into account is shown in Figure 4. Additionally, Figure 4 shows that the dependability indices rise when the average pole diameter and reinforcement ratio rise, respectively. Increases in average diameter and reinforcement ratio may result in higher reliability indices since they improve moment capacity, which in turn raises the dependability of reinforced concrete poles. This pattern is consistent with the findings of Quadri and Afolayan (2017). Figure 4 shows that only at reinforcement ratios of 2.75 and 3.0, which correspond to average pole diameters of 500 mm and 495 mm, respectively, is the necessary goal dependability index of 3.8 fulfilled.

Given the concrete capacity under strain, Figure 5 illustrates the link between the assumed reliability indices and the characteristic strength of reinforcement for different values of the reinforcement ratio. Additionally, Figure 5 shows that the dependability indices rise in tandem with increases in the reinforcement ratio and characteristic strength of reinforcement, respectively. This tendency is consistent with Quadri and Afolayan (2017). The rise in reliability indices with increases in the characteristic strength of reinforcement and the reinforcement ratio may be the result of an increase in moment capacity, which raises the reliability of reinforced concrete poles.

The link between the area of tension reinforcement and the indicated dependability indices at different lengths of reinforced concrete poles while taking concrete capacity in tension into account is shown in Figure 6. Additionally, Figure 6 shows that the dependability indices rise as the area of tension reinforcement grows and fall as the pole length increases. This pattern is consistent with Quadri and Afolayan (2017) and suggests that the rise in reliability indices with an increase in the area of tension reinforcement may be the result of an increase in moment capacity, which raises the reliability of reinforced concrete poles. One possible explanation for the decline in pole dependability as pole length increases is an increase in the bending moment on the reinforced concrete pole, which results in a commensurate decline in the pole's reliability.

The link between the assumed dependability indices and typical wind load for different reinforced concrete pole lengths, taking into account the concrete capacity in tension, is shown in Figure 7. Additionally, Figure 7 shows that the dependability indices drop as the typical wind load increases and as the length of the reinforced concrete pole increases, respectively. Because increasing pole length and typical wind load both increase the bending force on the pole, dependability indices fall as both factors grow. This pattern is consistent with the findings of Quadri and Afolayan (2017). Since they meet the necessary goal dependability index of 3.8, Figure 7 shows that the pole is safe for typical wind loads of 19 KN, 24 KN, 36.5 KN, and 68 KN, which correspond to pole lengths of 6 m, 4.5 m, 3 m, and 1.5 m, respectively.

The link between the length of the reinforced concrete pole and the assumed dependability indices at different effective depths of the reinforced concrete pole section, taking into account the concrete capacity under stress, is shown in Figure 8. Additionally, Figure 8 shows that the reliability indices rise as the effective depth reinforcement ratio grows and fall as the pole length increases, respectively. While the decrease in pole reliability with increasing pole length may be linked to an increase in bending moment on the pole, the increase in reliability indices with increasing effective depth and reinforcement ratio may

be caused by an increase in moment capacity, which in turn causes a corresponding increase in the reliability of reinforced concrete poles. This pattern is consistent with the findings of Quadri and Afolayan (2017). Since the necessary goal dependability index of 3.8 is met, Figure 4.8 shows that the pole is safe at effects of 1.1, 1.65ive depth values of 265mm, 220mm, 275mm, 330mm, 385mm, and 440mm, which correspond to pole lengths of 1.5m, 2m, 3m, 3.75m, 4.5m, 5.5m, and 6.5m, respectively (EN,1990).

The link between the length of the reinforced concrete pole and the suggested dependability indices at different characteristic reinforcement strength values while taking the concrete's capacity in tension into account is shown in Figure 9. Additionally, Figure 9 shows that the reliability indices rise as the characteristic strength of reinforcement grows and fall as the pole length increases, respectively. This pattern is consistent with the findings of Quadri and Afolayan (2017). While the reliability of reinforced concrete poles decreases with increasing pole length, this decrease can be linked to an increase in bending moment on the pole. The increase in reliability indices with increasing characteristic strength of reinforcement may be caused by an increase in moment capacity.

The link between the length of the reinforced concrete pole and the assumed dependability indices for different concrete characteristic strength values, taking concrete capacity in compression into account, is shown in Figure 10. Additionally, Figure 10 shows that the dependability indices rise as concrete's characteristic strength grows and fall as pole length increases, respectively. This pattern is consistent with the findings of Quadri and Afolayan (2017). While the reliability of reinforced concrete poles decreases with increasing pole length, this decrease can be linked to an increase in bending moment on the pole. The increase in reliability indices with increasing concrete characteristic strength may be caused by an increase in moment capacity.

The link between the assumed dependability indices and typical wind load for different reinforced concrete pole lengths, taking into account the concrete's capacity in compression, is shown in Figure 11. Additionally, Figure 11 shows that the reliability indices decrease as the characteristic wind load and pole length of the reinforced concrete pole increase, respectively. This trend is consistent with Mustapha and Abejide's (2019) findings that the reliability indices decrease as the characteristic wind load and pole length increase because these factors both increase the bending moment on the pole. Given that they meet the necessary goal dependability index of 3.8, Figure 11 shows that the pole is safe for typical wind loads of 24 KN and 47 KN, which correspond to pole lengths of 3 m and 1.5 m, respectively.

The link between the average diameter of a reinforced concrete pole section and the associated reliability indices at different pole length values while taking concrete capacity in compression into account is shown in Figure 12. Additionally, Figure 12 shows that the dependability indices rise as the average pole diameter grows and fall as the pole length increases, respectively. This pattern is consistent with Quadri and Afolayan's (2017) assertion that reliability indices rose as average diameter increased. This might be because higher moment capacity leads to a comparable rise in reinforced concrete pole dependability. Given concrete capacity in compression, Figure 13 illustrates the link between the assumed dependability indices and the effective depth of the reinforced concrete pole section at different lengths. Additionally, Figure 13 shows that the dependability indices rise as effective depth grows and fall as pole length increases, respectively. As can be seen from Figure 13, the pole is safe at effective depths of 275mm, 330mm, 430mm, and 495mm corresponding to pole lengths of 1.5m, 3m, 4.5m, and 6m respectively, as the required target reliability index of 3.8 is satisfied. This trend is consistent with Quadri and Afolayan's (2019) findings that the reliability index increased with effective depth and reinforcement ratio. This could be due to an increase in moment capacity, which causes a corresponding increase in the reliability of reinforced concrete pole.

The connection between the assumed reliability indices and characteristic wind load at different area per link reinforcement spacing values, taking into account the failure of reinforced concrete poles under shear, is shown in Figure 14. Additionally, Figure 14 shows that the dependability indices rise with increasing area per spacing of link reinforcement and fall with increasing typical wind load, respectively. When characteristic wind load increases, the bending moment on the pole increases, which is why

reliability indices decrease. Conversely, when area per link reinforcement increases, the shear capacity of the reinforced concrete pole increases, which is why reliability indices increase.
The link between the inferred reliability indices and characteristic wind load at different reinforcement ratio values, taking into account the failure of reinforced concrete poles in shear, is shown in Figure 15. Additionally, as shown in Figure 15, the reliability indices decline when the typical wind load and reinforcement ratio rise, respectively. As the characteristic wind load on the pole increases, the bending moment on the pole increases as well, which is why reliability indices decrease as the reinforcement ratio increases. Conversely, when the reinforcement ratio increases, the values of the tension reinforcement also increase, increasing pole reliability. The pole is safe at reinforcement ratios of 0.55, 1.1, 1.65, 2.2, 2.75, and 3.0, as shown in Figure 15. These values correspond to typical wind loads of 59, 60, 61, 62, 63, and 64 KN, respectively, because the necessary dependability index of 3.0 is satisfied.
When taking into account the failure of a reinforced concrete pole in shear, Figure 16 illustrates the link between the assumed reliability indices and characteristic wind load at different areas of tension reinforcement. Additionally, Figure 16 shows that the dependability indices rise with an increase in the area of tension reinforcement and fall with an increase in typical wind load. When characteristic wind load on the pole increases, the bending moment on the pole increases as well, which is why reliability indices decrease as characteristic wind load increases. Conversely, when pole reliability increases with an increase in the area of tension reinforcement ratio, the values of the tension reinforcement also increase, increasing pole reliability. The pole is safe for all regions of tension reinforcement when the requisite reliability index of 3.0 is satisfied, as shown in Figure 16 for a representative wind load of 61.5KN.
Taking into account the failure of reinforced concrete poles in shear, Figure 17 illustrates the link between the assumed reliability indices and characteristic wind load for different values of the effective depth of the reinforced concrete pole section. Figure 17 further shows that the reliability indices rise with an increase in the effective depth of the reinforced concrete pole section and fall with an increase in the typical wind load. This pattern is consistent with Quadri and Afolayan's (2017) finding that the reliability index declined as characteristic wind load increased. This is because higher characteristic wind load on the pole results in a greater bending moment on the pole, and higher effective depth increases the moment capacity of the reinforced concrete pole section, which in turn increases pole reliability. The pole is safe for effective depths of 165, 220, and 275 mm, which correspond to typical wind loads of 44, 59, and 68 KN, respectively, as shown in Figure 17, because the necessary goal dependability index of 3.8 is met. Although it is safe, it is not cost-effective to install reinforced concrete poles deeper than 275 mm.
The link between the assumed dependability indices and characteristic wind load at different reinforced concrete pole lengths, taking concrete capacity in deflection into account, is shown in Figure 18. Additionally, Figure 18 shows that the dependability indices drop as the typical wind load increases and as the length of the reinforced concrete pole increases, respectively. Because increasing pole length and typical wind load both increase the bending force on the pole, dependability indices fall as both factors grow. Because they meet the necessary goal dependability index of 3.8, Figure 18 shows that the pole is safe for typical wind loads of 26.5KN and 47KN, which correspond to pole lengths of 6m and 4.5m, respectively.

CONCLUSION

According to the guidelines of BS 8110, 1997, the reliability study of a reinforced concrete pole in bending, shearing, and deflection, respectively, using MATLAB is taking into account the pole's failure in bending, shearing, and deflection, respectively, the reliability indices typically declined as the characteristic wind load and length of the reinforced concrete pole increased.
Taking into account the failure of reinforced concrete poles in bending, the pole is typically safe at reinforcement ratios of 1.65, 2.2, 2.75, and 3.0, which correspond to characteristic wind loads of 21.5 KN, 29 KN, 36.5 KN, and 40 KN, and considering the failure of reinforced concrete poles in bending, the pole is typically safe at reinforcement ratios of 1.1, 1.65, 2.2, 2.75, and 3.0, which correspond to effective depths of 495 mm, 415 mm, 365 mm, 315 mm, and 300 mm, respectively.

RECOMMENDATIONS

Based on the results obtained from the study, the following recommendations are hereby made: For good performance, the length of the reinforced concrete pole should not exceed 6m.

i. The effective depth of the reinforced concrete pole should not be less than 165mm.

ii. The computer programs developed in this study is suitable for reliability analysis of reinforced concrete pole, steel pole and timber pole respectively.

REFERENCES

Afolayan, J. O., (1997). Evaluation of the Economic Efficiency of the BS449 Design Criteria for Plate Girders. Journal of Engineering and Applied Sciences, 16(1), pp. 49-54.

Baghmisheh, A.G. and Mahsuli, M. (2021) 'Seismic performance and fragility analysis of power distribution concrete poles', *Soil Dynamics and Earthquake Engineering,* Vol. 150. Doi: 10.1016/j.soildyn.2021.106909.

British Standard Institution, BS 8110 Structural use of Concrete. Part 1 Code of Practice for Design and Construction. British Standard Institution, 1997.

Choi, S. K., Grandhi, R. V. & Canfield, R. A. (2006). Reliability-based Structural Design. 1st ed. London: Springer.

Dheenadayalan, B., (2003). Reliability Based Local-Global Design Optimization of Structures, Toledo: The University of Toledo.

Mustapha, A. and Abejide, O.S. (2019). Probabilistic Strength of Steel Poles used for production and transmissions. Reliability Engineering and Resilience 1(1), 29-41.

Oyetola, E.B. and Oritola, S.F. (2006) 'Investigation into the causes of electric transmission concrete pole failures', Leonardo Electronic Journal of Practices and Technologies, pp.17-24.

Phrommarat, B. and Arromdee, P. (2019) 'A life cycle assessment study of pre-stressed concrete poles in Thailand', *International Journal of Construction Management,* pp.1-12.

Quadri A. I. and Afolayan J. O. (2017). Reliability Assessment of Axial Load Effect on Electric Power Distribution Concrete Poles in Southwest Nigeria. International journal of scientific and Engineering research, 8(5), pp. 358-365.

Quadri, A. (2019) 'Reliability appraisal of nominal eccentricity of short reinforced concrete column designed to BS 8110 and Eurocode (EN: 2)-ultimate limit state on fatigue', Reliability Engineering

Sankey, B. and Crisp, M.H.T. (1921) 'Reinforced concrete poles for overhead line and traction work', Transactions of the South African Institute of Electrical Engineers, Vol. 12, pp.175-175.

Sule, S. and Benu, M.J. (2019). Reliability Analysis of a solid timber column subjected to axial and lateral loading, FUOYE Journal of Engineering and Technology, 4 (2), 1-5.

Thoft-Christensen, P. & Baker, M. J. (1982). Structural Reliability Theory and its Applications. Berlin: Springer-Verlag.